



Studies of the nonthermal electrons in high density plasma in the T-10 tokamak

P.V.Savrukhin, A.V.Sushkov

RRC Kurchatov Institute, Moscow, Russia



9th IAEA Technical Meeting on Energetic Particles in
Magnetic Confinement Systems

November 10, 2005, Takayama, Japan





Outline

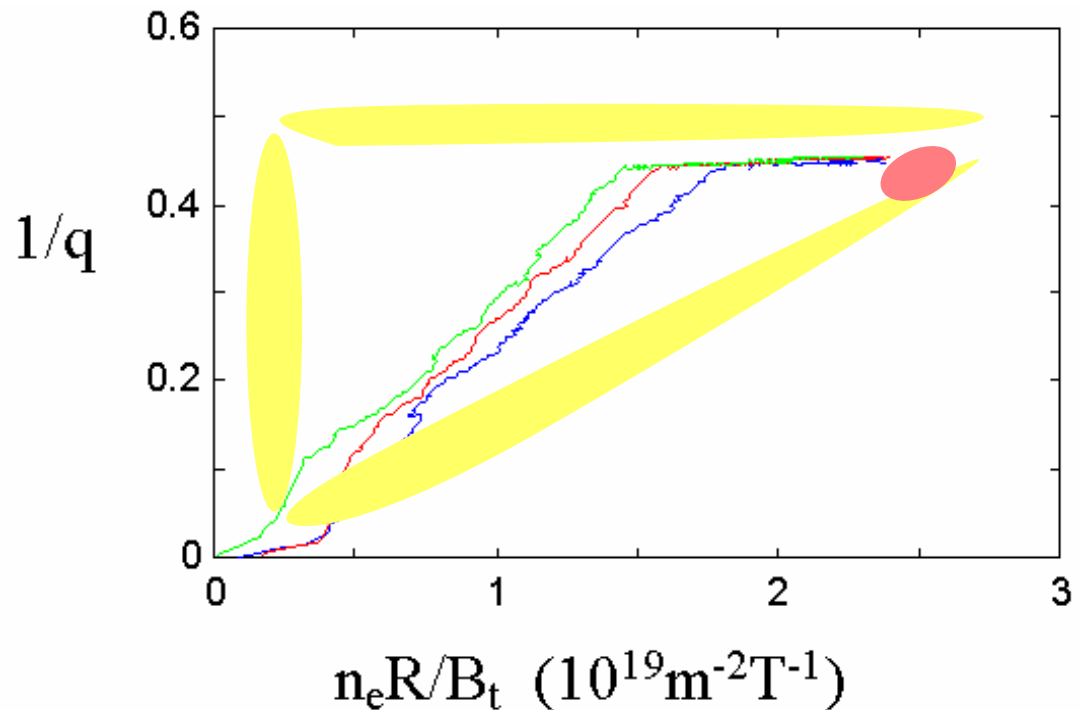
- **Introduction** (*nonthermal electrons and plasma disruption*)
- **Diagnostic techniques**
- **Experimental studies**
- **Summary**



Non-thermal electrons in tokamaks

Non-thermal electrons are observed in previous experiments in tokamaks

- in plasma with **low density**
- at the **initial stage** of the discharge ,
- during **powerful auxiliary heating**,
- during/after **major disruptions** ●



High-density OH plasma is considered in present experiments

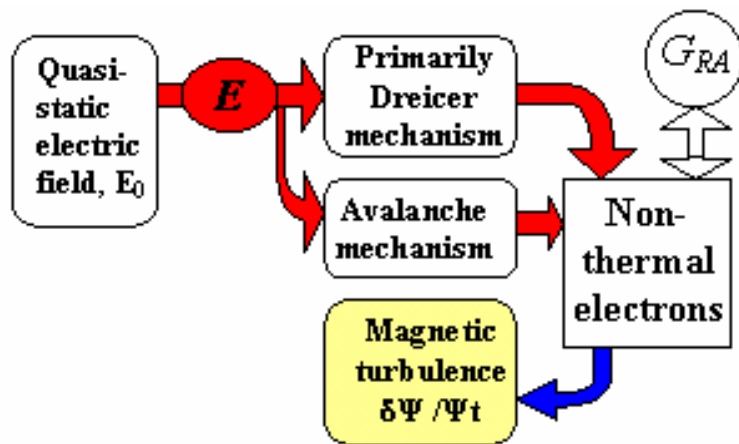
Effect of standard runaway formation can be neglected



“...Extensive experimental and theoretical studies have identified physics basis of runaway formation, loss and wall interaction in both present and reactor scale tokamaks...”

[ITER,NF99]

$$\frac{\partial N_r}{\partial t} + \nabla \cdot (\mathbf{v}_r N_r) = n_e / \tau_{dr} + N_r / \tau_{av} - \nabla \cdot \Gamma_{loss}$$

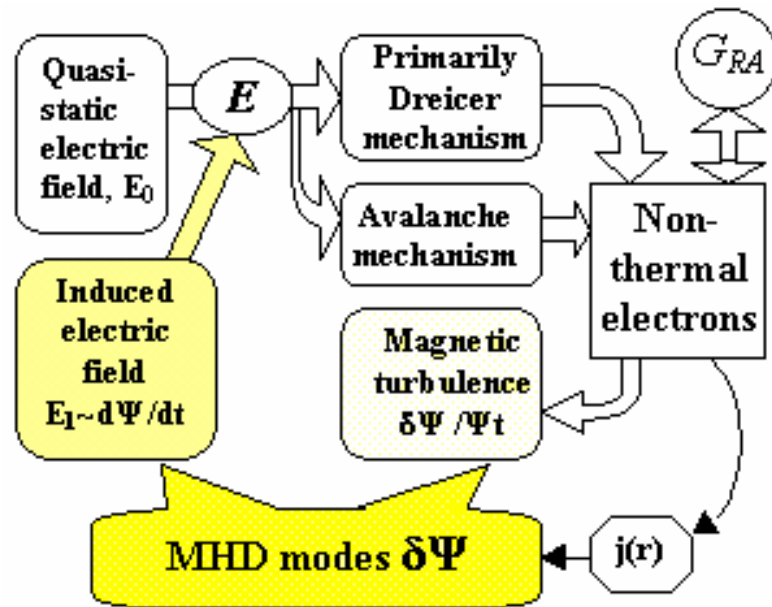


Growth of the runaway avalanches depends critically on the primary population of the fast electrons

✓ *The primary beam formation is generally believed to be connected with Dreicer electron acceleration in longitudinal electric field after an energy quench*



Analysis have indicated, however, that primary electron acceleration can be connected with strong electric fields (E up to 50 V/m) induced during magnetic reconnection



$$dN_r/dt = n_e/\tau_{dr} + N_r/\tau_{av} - N_r/\tau_{loss}$$

$$\tau_{dr}^{-1} \approx 0.3 v_e \epsilon_d^{-3(Z_{eff}+1)/16} \exp(-1/4\epsilon_d - ([Z_{eff}+1]/\epsilon_d)^{1/2})$$

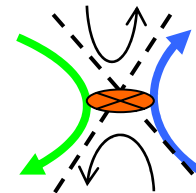
$$\epsilon_d = E/E_c \quad E_c = e^3 n_e Z_{eff} \ln \Lambda / (4\pi \epsilon_0^2 m_e v_{th}^2)$$

$$\tau_{av}^{-1} \approx eE / 2m_e c \ln \Lambda a(Z_{eff})$$

$$\tau_{loss}^{-1} \approx D_m / \delta r^2 \quad D_m \approx (\pi R_0 q v_r) (\delta B/B_i)^2 \quad \delta r \sim w_1$$

$$\delta B/B_i = s_1 w_1^2 / (16 r_1 (R_0 + r_1))$$

$$E_1 \sim (1-q_0) r_1 B_{p1} / 4t_{crash}$$



MHD modes :

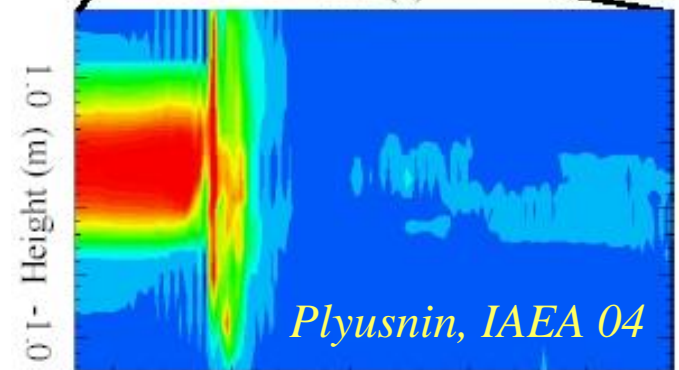
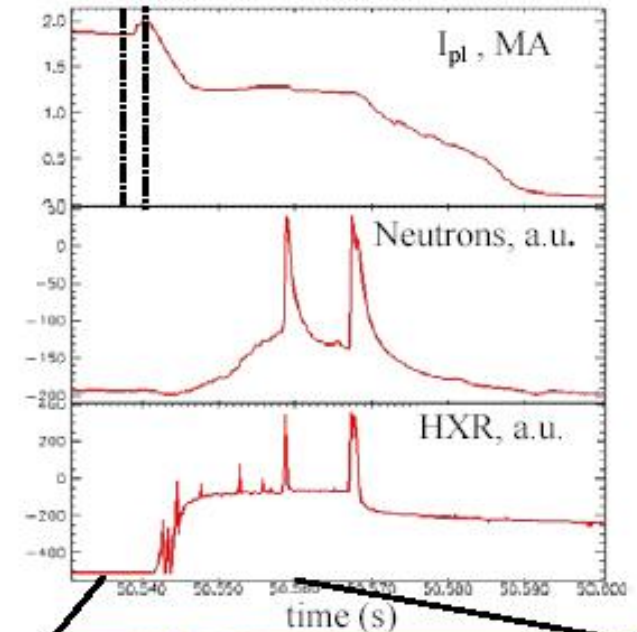
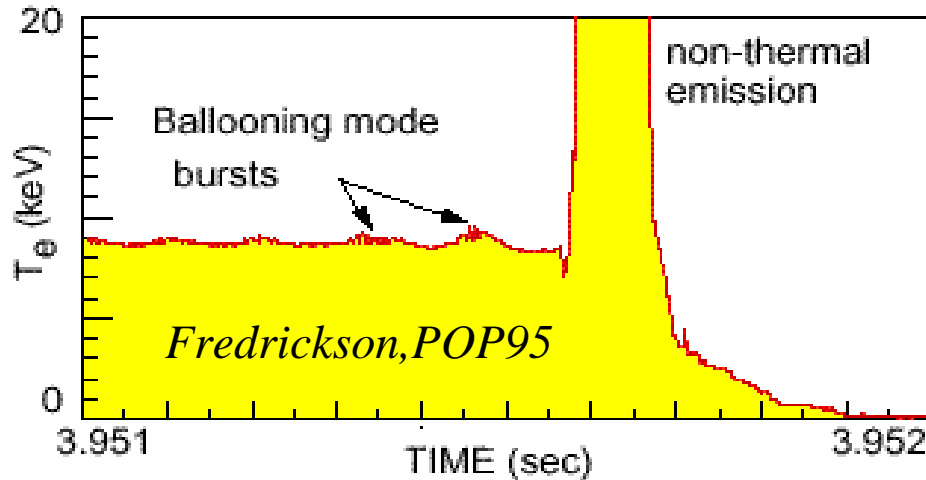
- are considering generally as a source of magnetic turbulence and loss mechanism of the runaway electrons
- can in fact provide seed population of non-thermal beams with subsequent formation of the strong runaway avalanches

Non-thermal electrons and disruptions

Acceleration of electrons to suprathermal energies, $E_{\gamma} \sim > 100 \text{keV}$, is a typical feature of plasma disruptions

- **disruptions at high I_p, B_+ (JET)**
 $I_{RA} \sim 0.6 I_p$

- **disruptions at high beta (TFTR)**



Previous experiments:

Detailed analysis of the precursor perturbations
Scattered data on the post-quench analysis

RADIATIVE DENSITY LIMIT DISRUPTION IN T-10 OHMICALLY HEATED PLASMA

T01-25855

electron density, radiated power

Additional gas puff

Enhanced radiation at the plasma edge

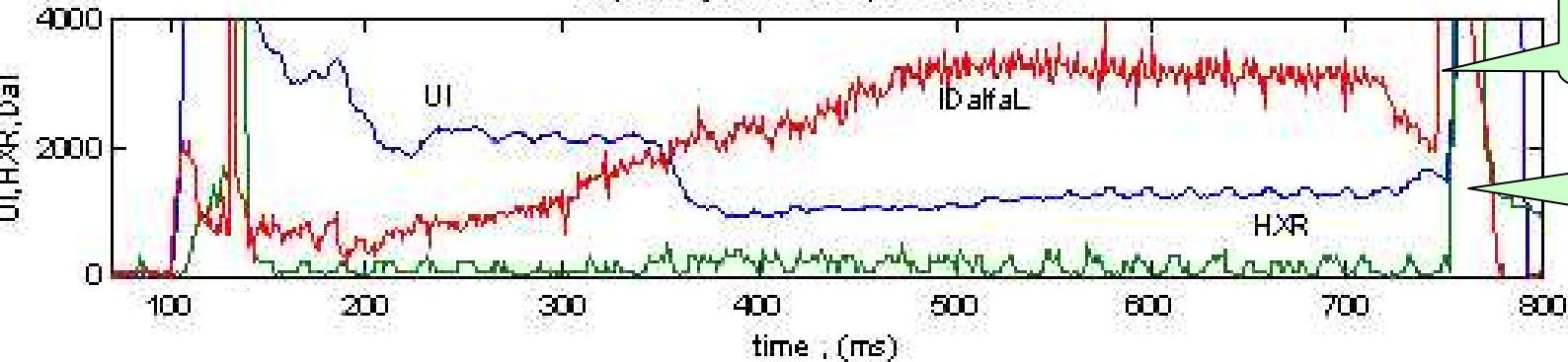
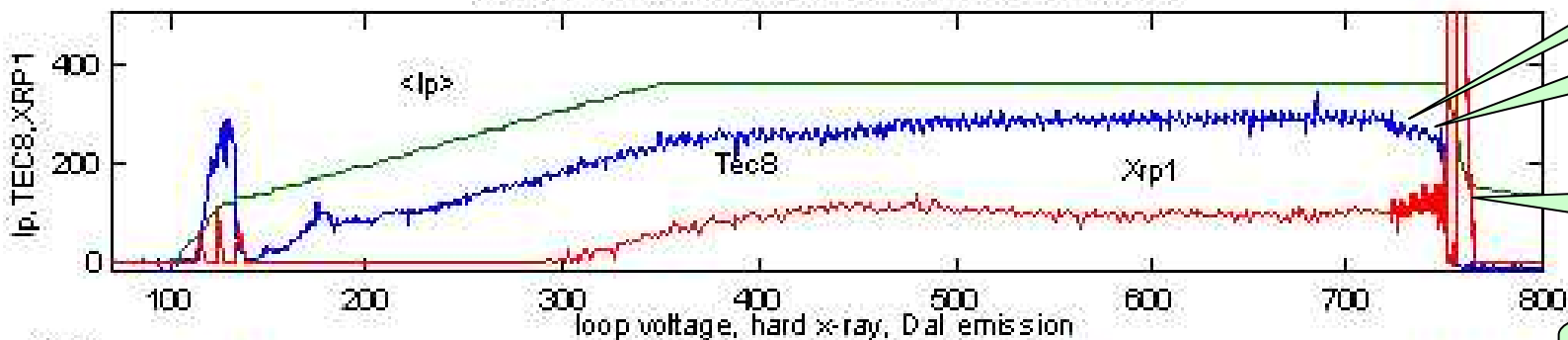
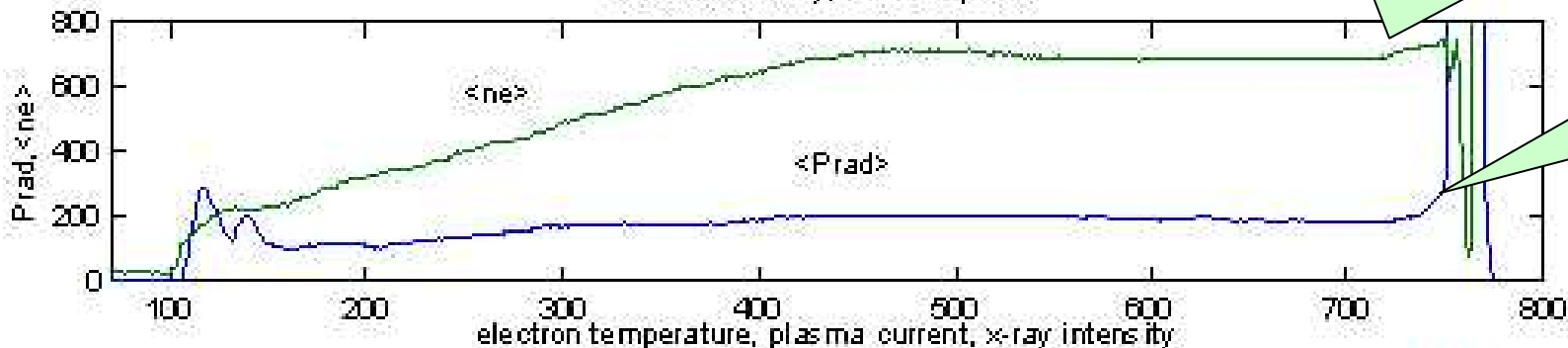
$T_e(r)$ erosion

2/1&1/1 modes

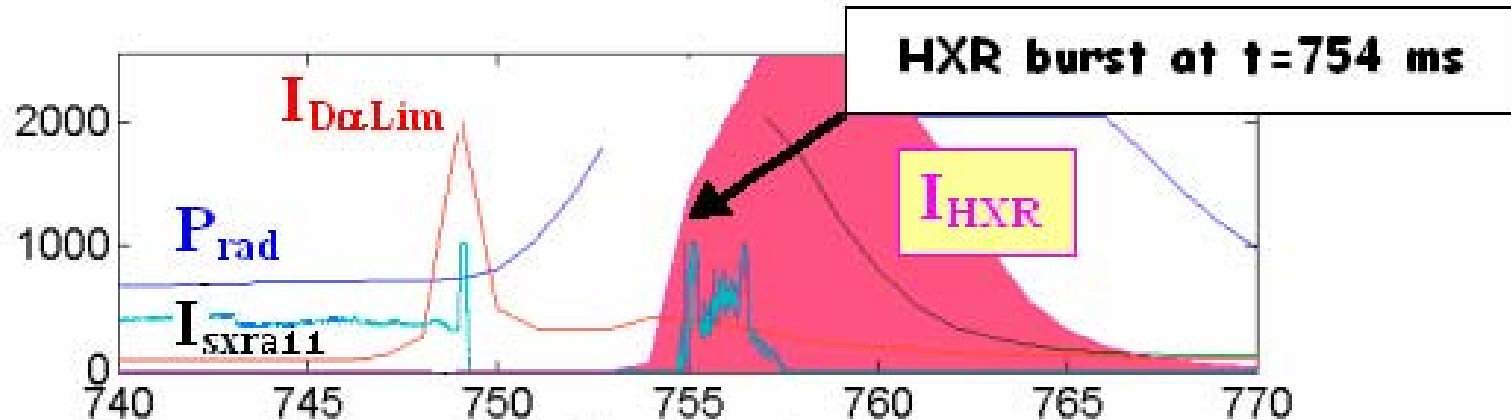
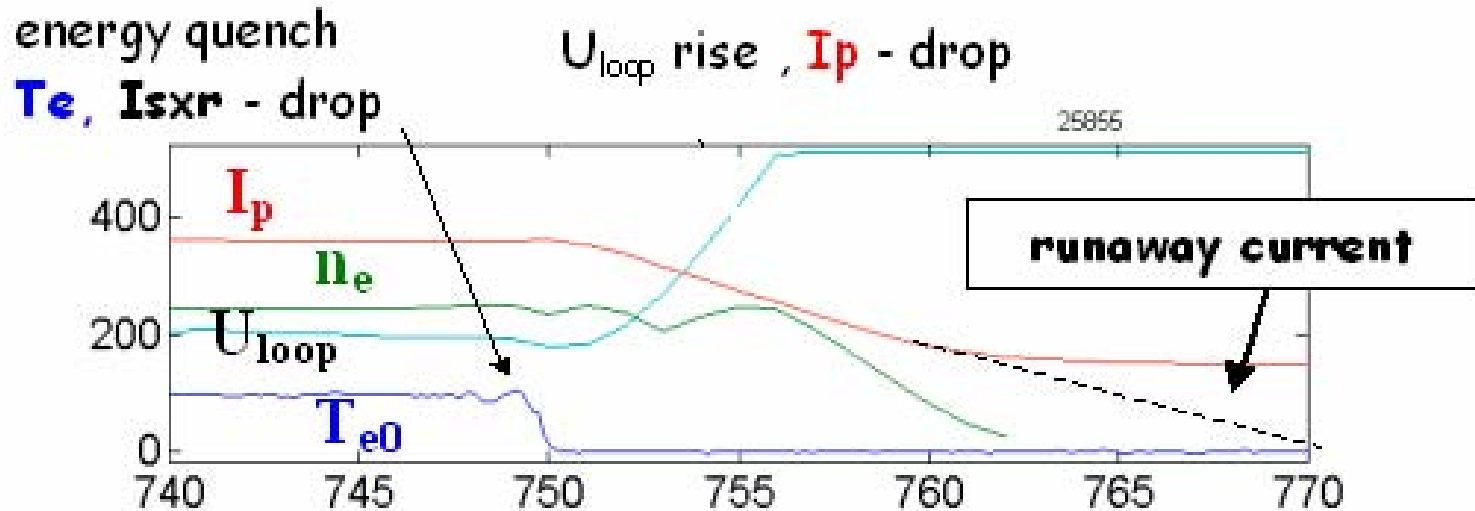
Energy quench

Loop voltage growth

HXR burst runaways



Standard hard x-ray burst are observed 5ms AFTER the energy quench during runaway interaction with the “wall”



Time (ms)

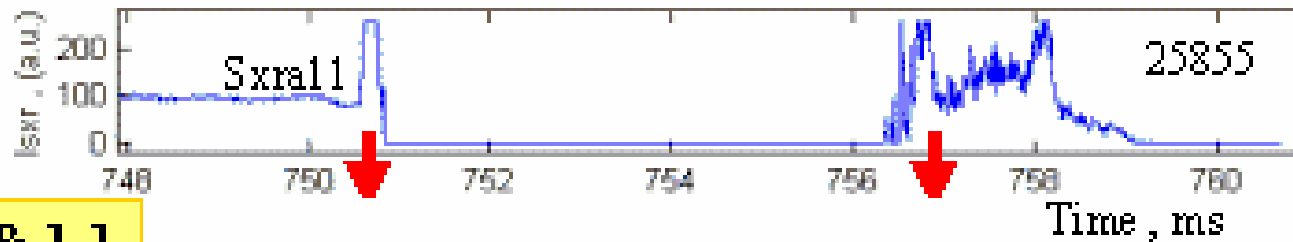
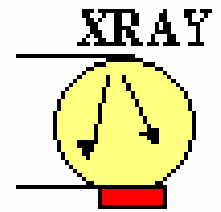
Stage I pre-disruptive

Stage II energy quench and runaway formation

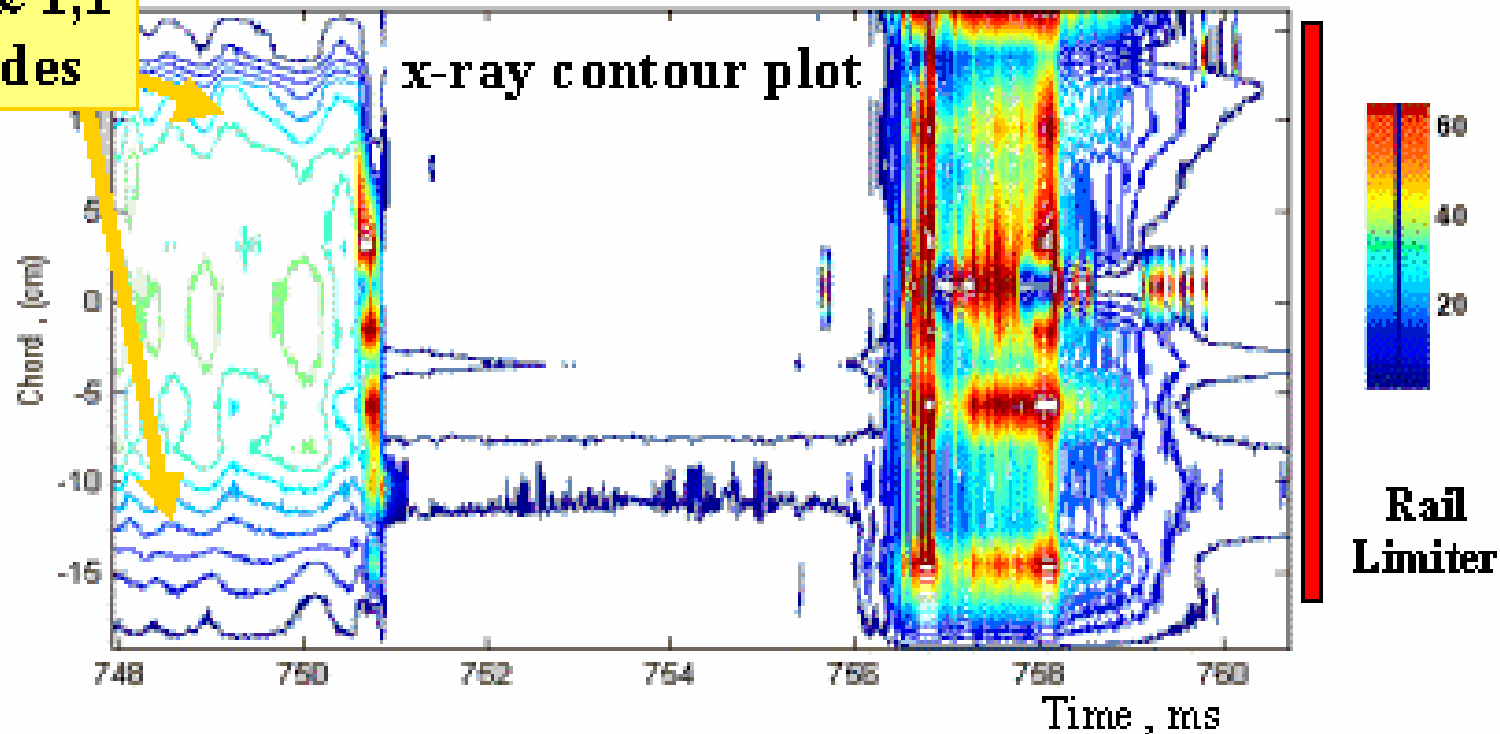
Stage III runaway avalanche



Structure of the bursts during runaway wall interaction can be identified using standard X-ray imaging systems with orthogonal view of the plasma column



2,1 & 1,1
modes

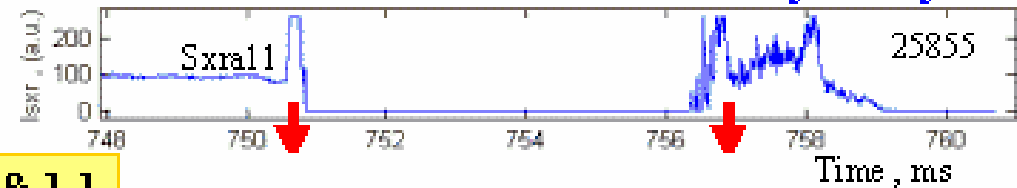
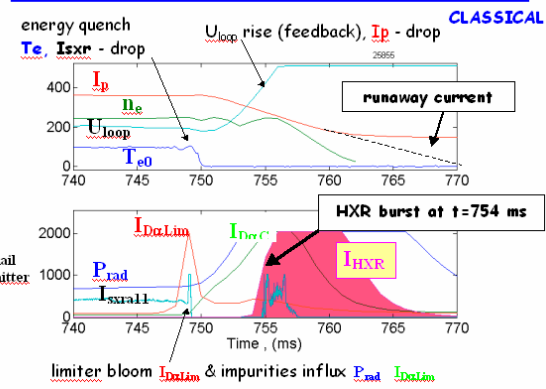


Identification of the non-thermal electrons in-flight is a complicated task

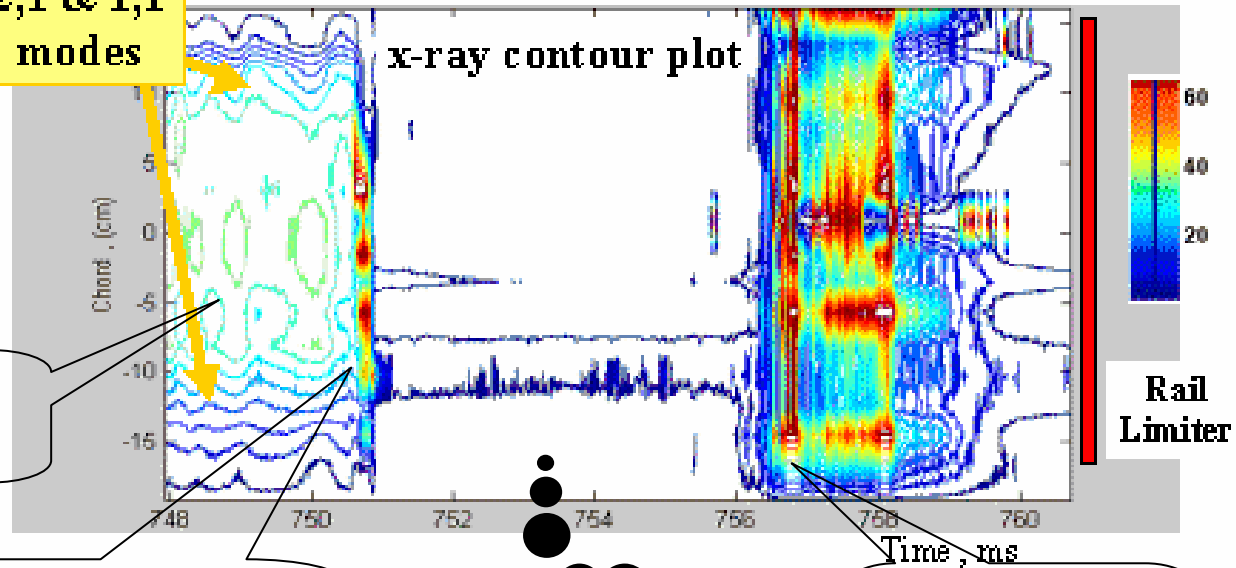
“Classical” hard x-ray bursts during density limit disruption

observed with conventional x-ray arrays

Hard x-ray burst (0.5-2.0MeV) - runaway electrons

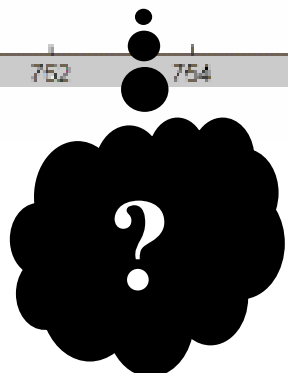


2,1 & 1,1 modes



Pre-disruptive plasma

X-ray spikes during the first energy quench



X-ray spikes during the runaway-wall interaction

Mystery of the runaway growth



Objectives of present experimental studies:

Analysis of formation and loss of the non-thermal electron beams during disruption instability in the T-10 tokamak

The following questions are addressed in the experiments

- What is the structure of the internal MHD perturbations at the onset of the non-thermal spikes?
- What is the origin of the primary non-thermal x-ray bursts observed during the first energy quench?
- What is the structure of the secondary x-ray bursts?
- What determines stability of the runaway beam?
- Characterisation of the runaway - wall interaction?

Do we have adequate diagnostics for reliable identification of the localized suprathermal electrons beams in a tokamak plasma?



Outline

- **Introduction**

- **Diagnostic techniques** *for studies of the nonthermal electrons during a disruption*

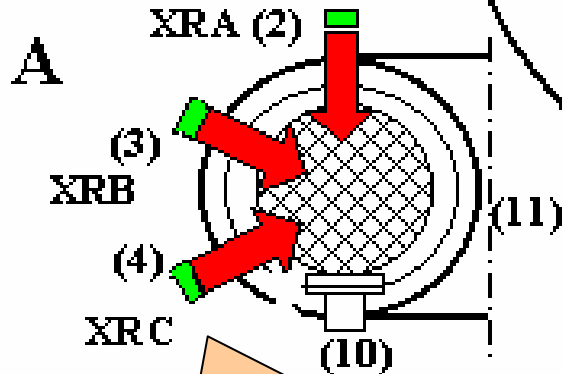
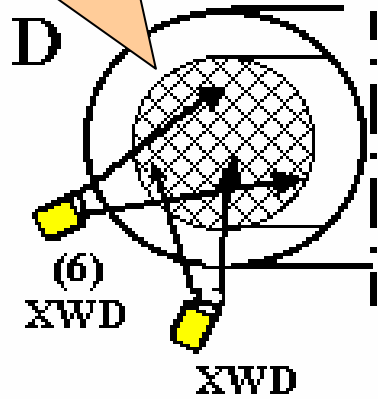
- **Experimental studies**

- **Summary**

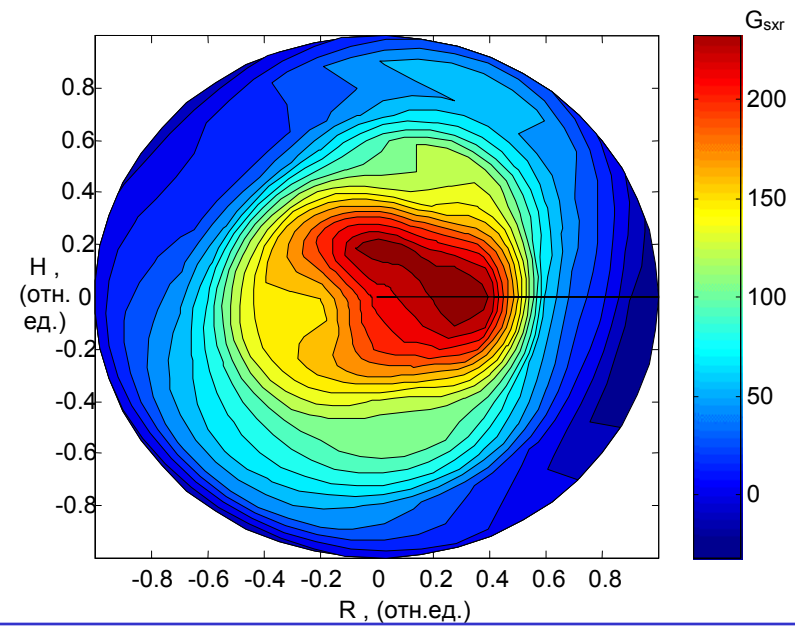
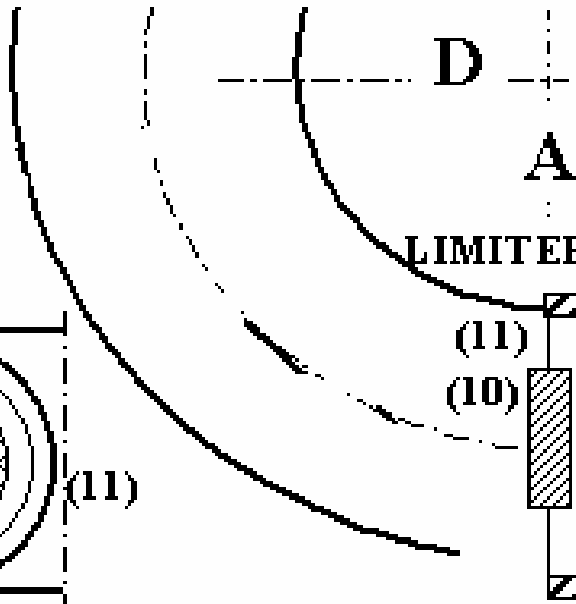
Internal structures of the MHD modes are identified in T-10 tokamak using soft x-ray tomographic imaging systems placed at two toroidal locations

- *Reliable tomographic reconstruction of the MHD modes (up to $m=2$)*
- *Limited energy range $E_\gamma < 15\text{keV}$*

x-ray gas detectors
XWD (32+32)

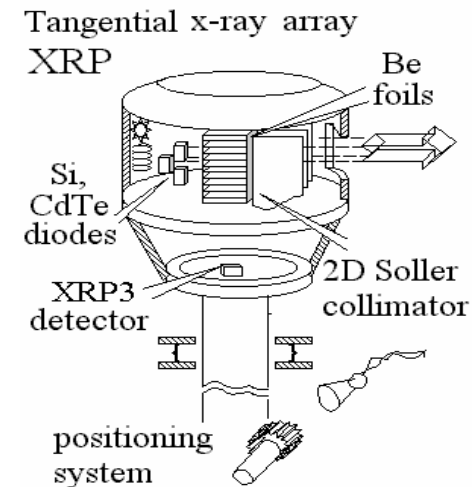
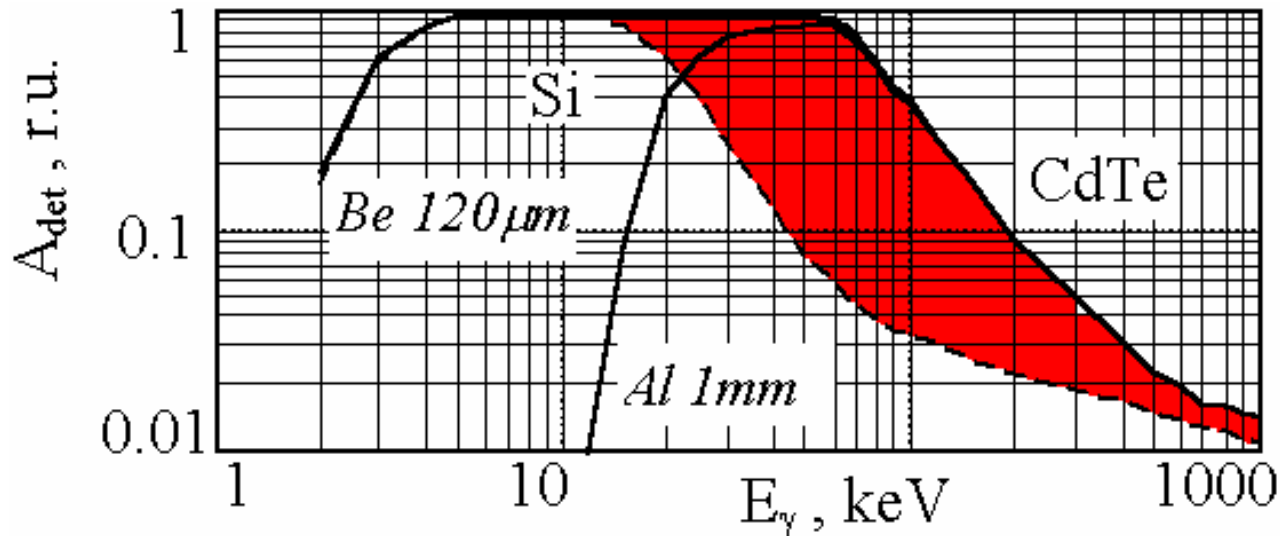


Si surface barrier tomographic arrays
(20+19+19 detectors)





CdTe detectors - enhanced sensitivity at 10 - 200 keV

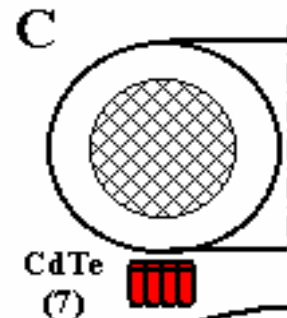
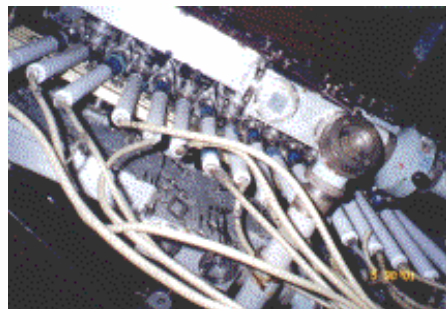


Rev. Sci. Instrum., 73 (2002) 4243
Rev. Sci. Instrum., 72 (2001) 1668

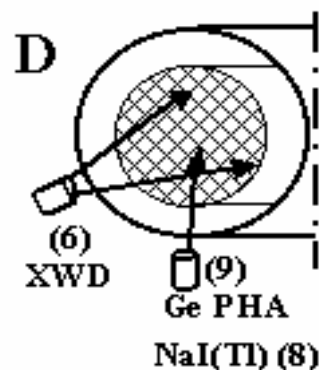


CdTe detectors with orthogonal view of the plasma column are placed at various locations around the torus

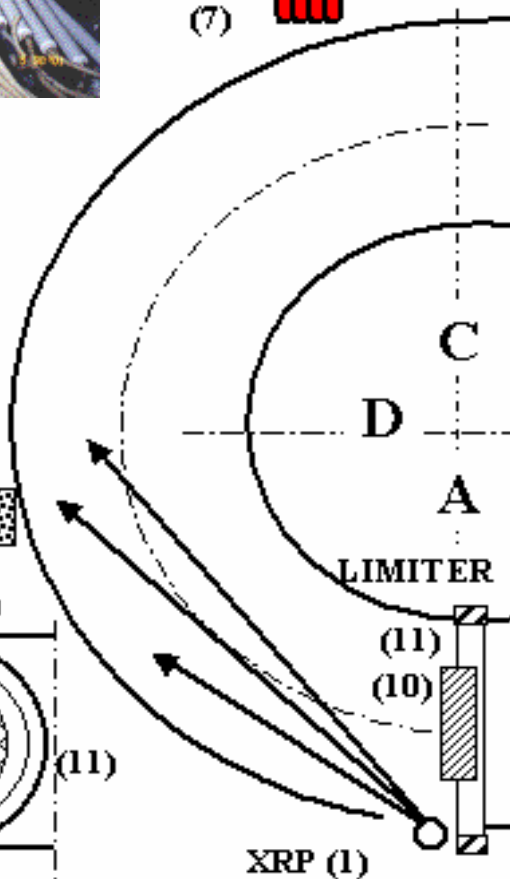
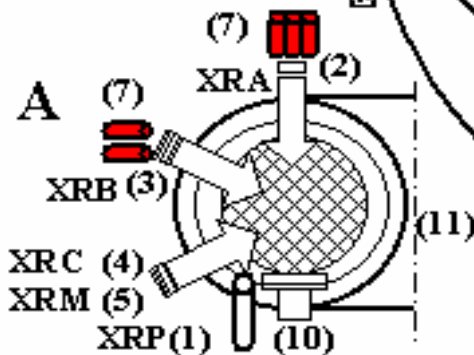
array of 16 detectors was placed temporarily at the interferometer waveguides ($E_\gamma > 40\text{keV}$)



array of 10 detectors vertical view $\Theta = +90^\circ$



array of 6 detectors vertical view $\Theta = +30^\circ$

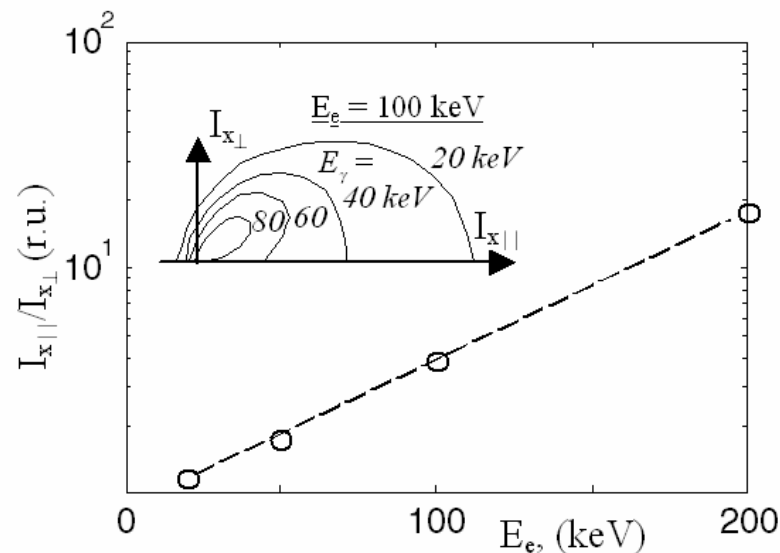
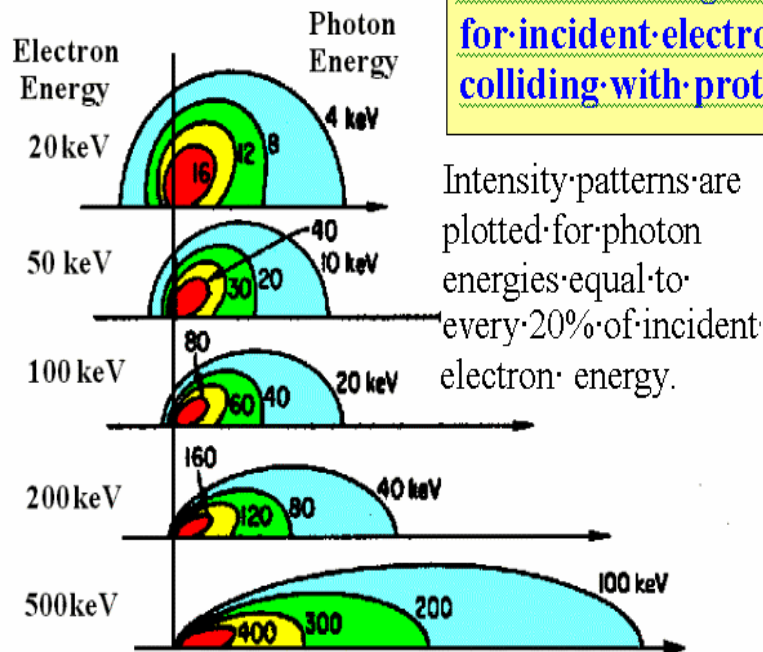




CdTe detectors with orthogonal view of the plasma column are insensitive to the non-thermal electrons with x-ray emission in limited forward cone along the electron lines of flight

S.VON GOELER et al.
Nucl. Fusion, 1985, 1515

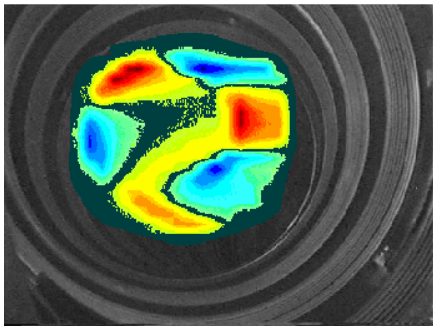
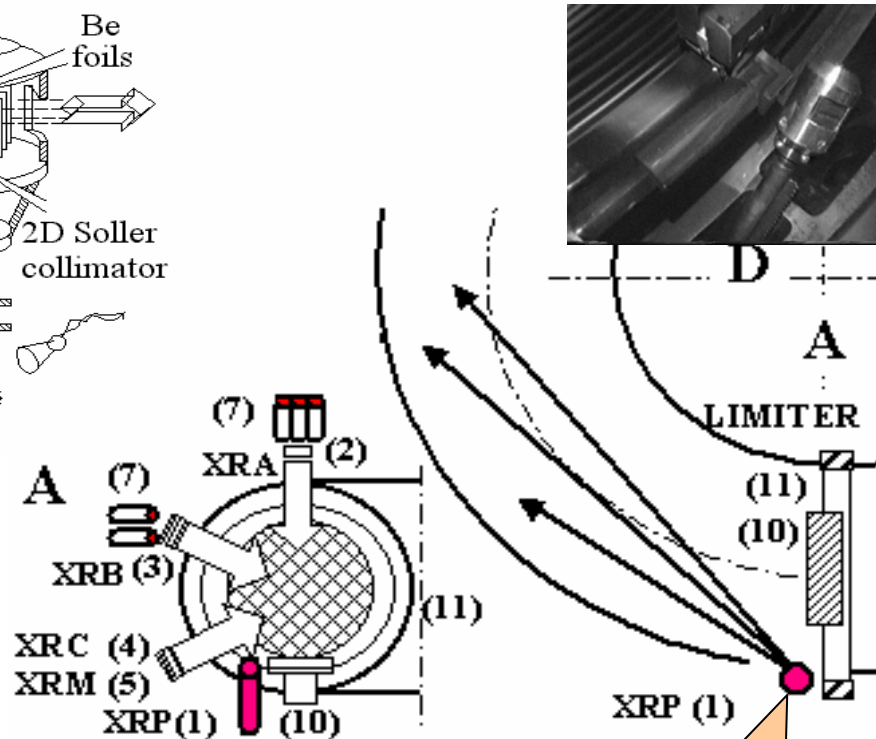
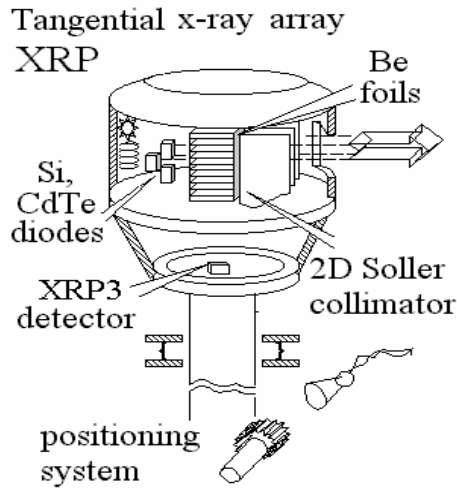
Polar plot
bremsstrahlung intensity
for incident electrons
colliding with protons



for original data see [S.VonGoeler, et al.,
Nucl. Fusion 25, (1985) 1515]

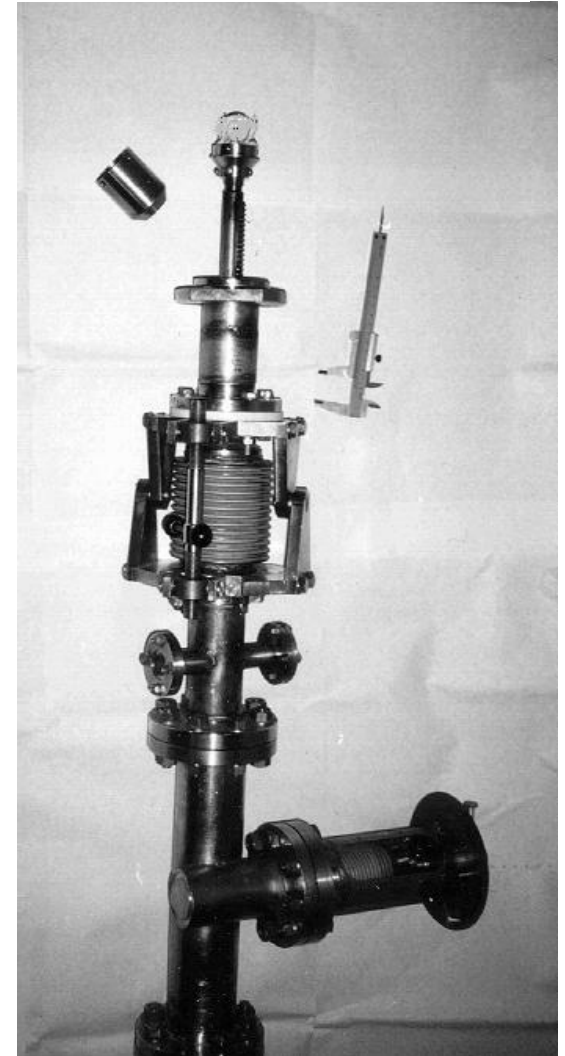
X-ray measurements in direction tangential to the plasma column can provide enhanced sensitivity to the non-thermal electrons

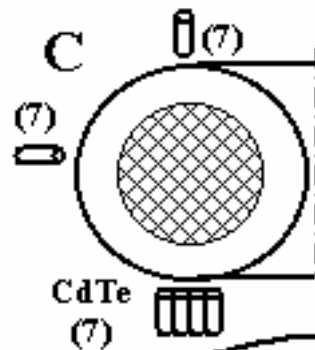
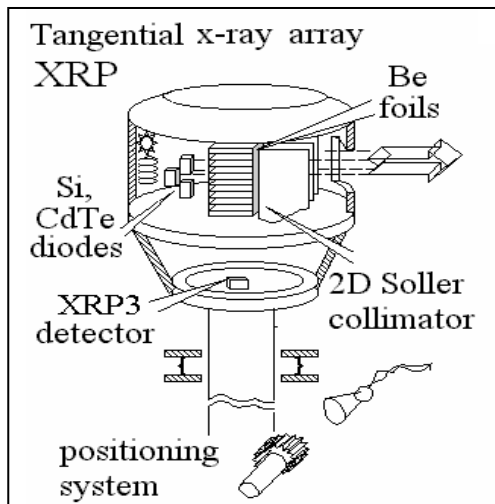
CdTe detectors with tangential view of the plasma column are placed inside the T-10 vacuum vessel



Tangential view (simulation)

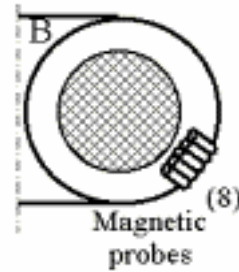
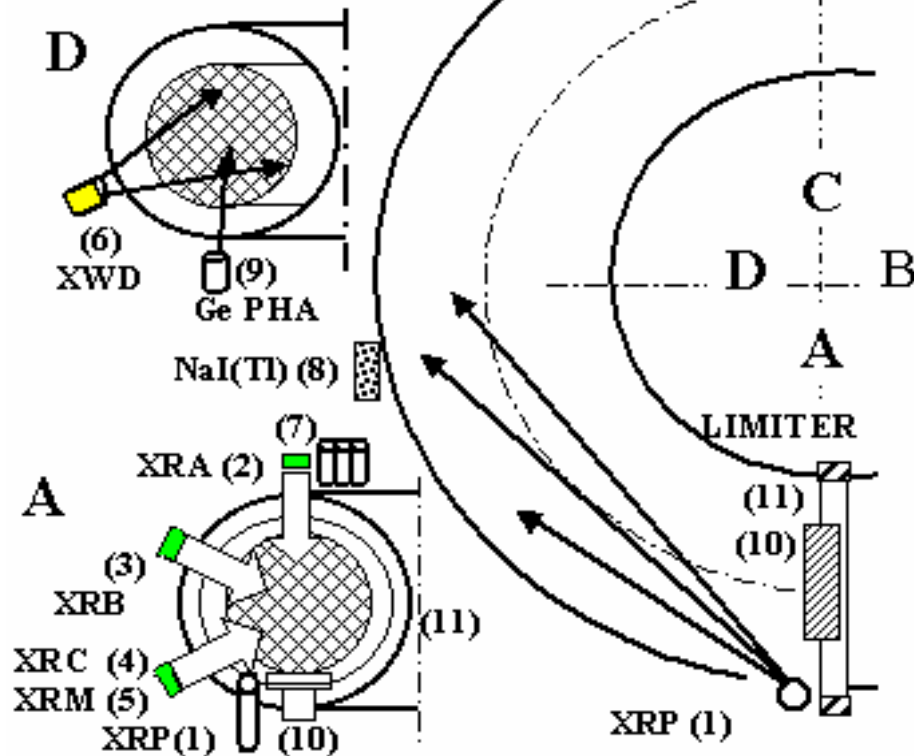
In-vessel array
3 Si and 1 CdTe
detectors





T-10 tokamak ($R=1.5, a=0.3\text{m}$)

- tangential x-ray array XRP (1),
- standard x-ray tomographic arrays XRA (2), XRB (3), XRC (4),
- x-ray matrix array XRM (5),
- x-ray gas detector XWD (6),
- sets of CdTe detectors (7).
- NaI(Tl) monitor (8) and
- Ge PHA system (9).





Outline

- Introduction
- Diagnostic techniques
- **Experimental studies**

Structure of the internal MHD perturbations at the onset of the non-thermal spikes

Origin of the primary non-thermal x-ray bursts observed during the first energy quench

Structure of the secondary x-ray bursts

Stability of the runaway beam

- **Summary**

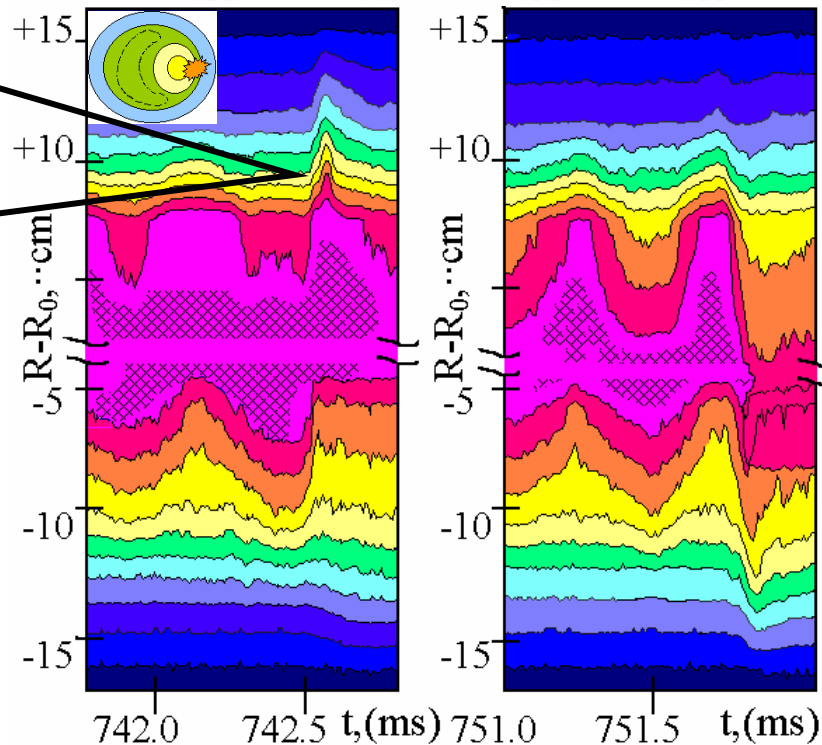
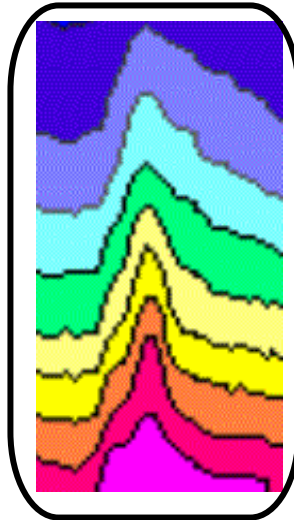
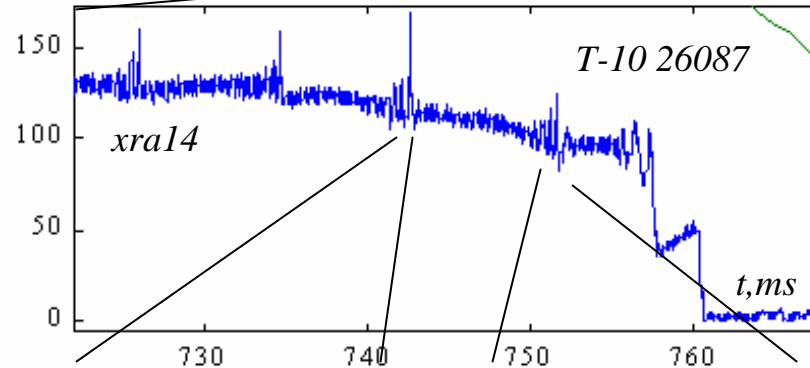
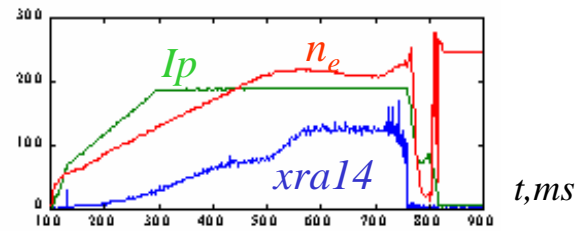


Energy quench at the density limit is proceeded by series of sawteeth

The sawteeth are accompanied with spikes (“rib”) superimposed with the $m=1$ mode

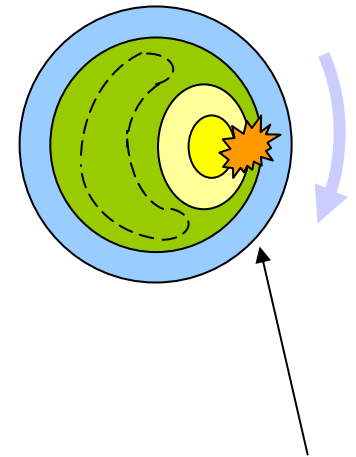
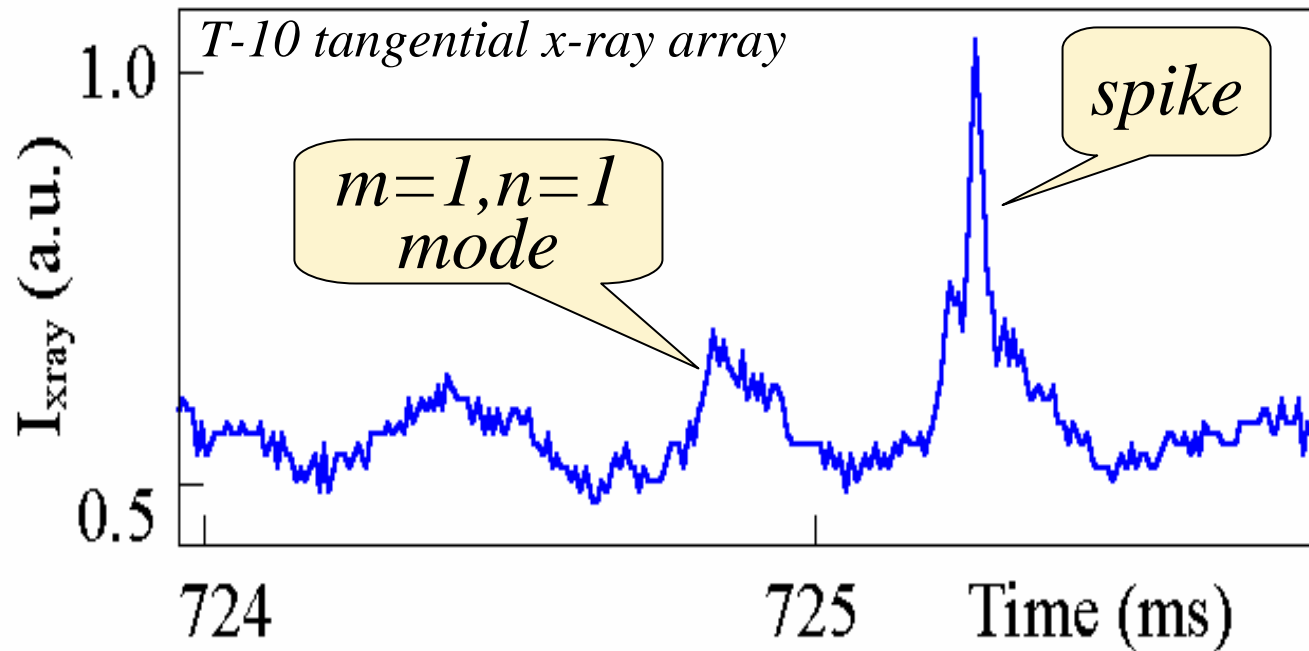
The spikes are observed at low and high field side of the torus

Observed previously in TFTR, DIII-D
E.Fredrickson, PP98



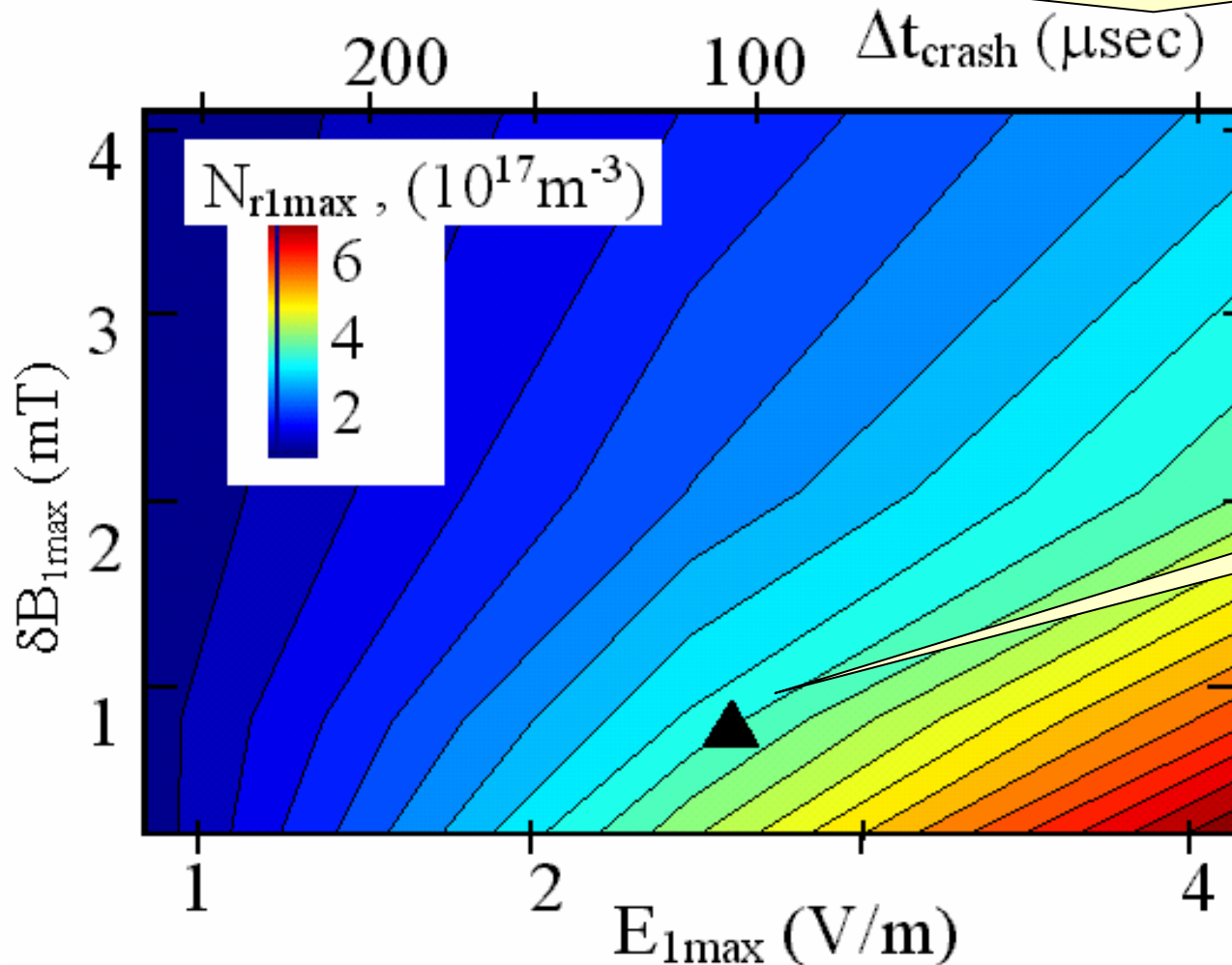


The non-thermal x-ray spikes are observed more clearly using tangentially viewing x-ray array



The spikes can be connected with generation of the non-thermal electrons during magnetic reconnection

Contour plot of the maximum non-thermal electron density (N_{r1max}) calculated in plasma with various amplitude of the induced electric field (E_{1max}) and magnetic field perturbations (δB_{1max}).

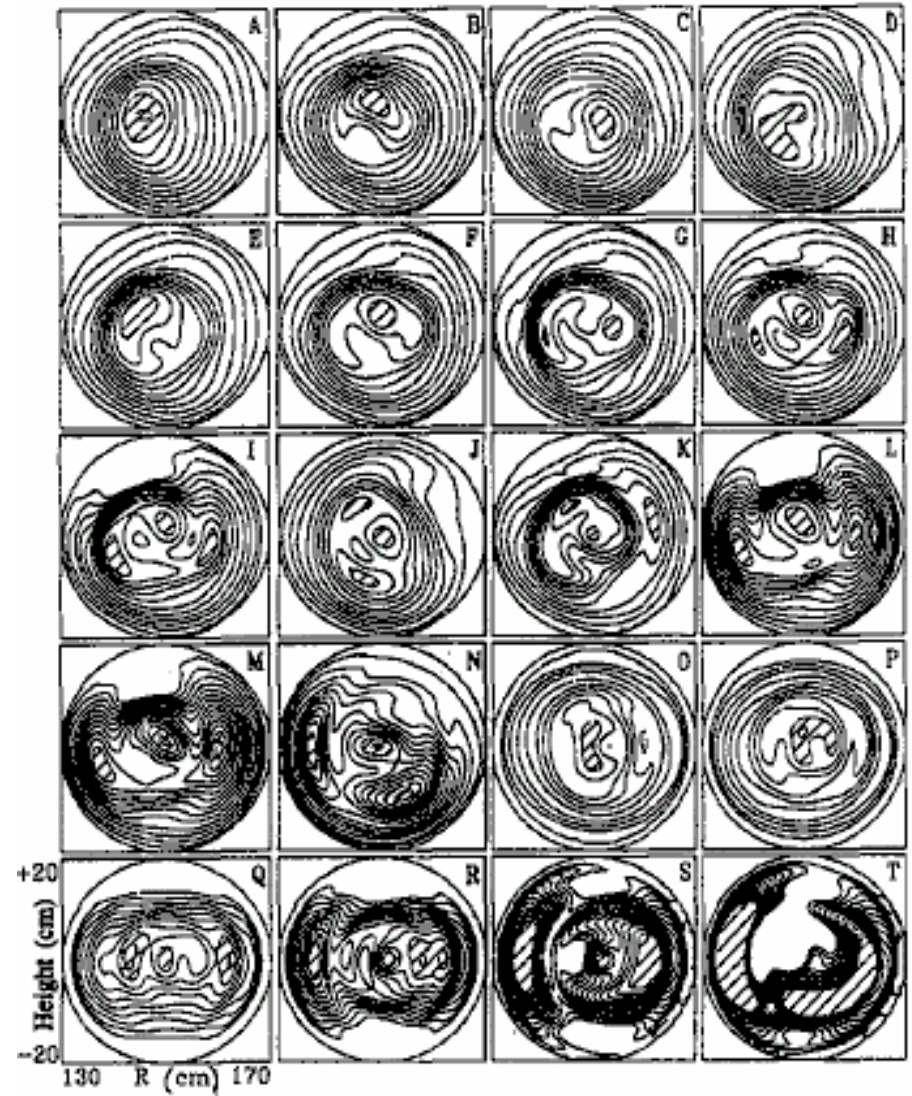
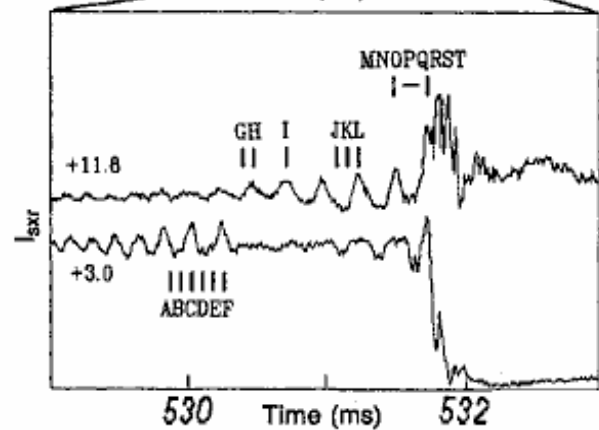
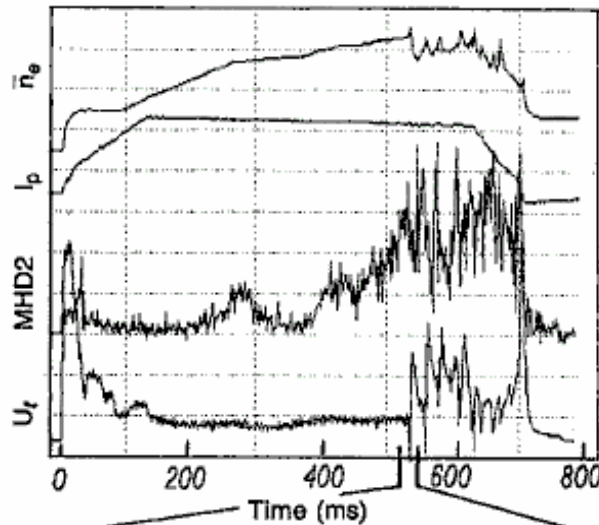


Typical set



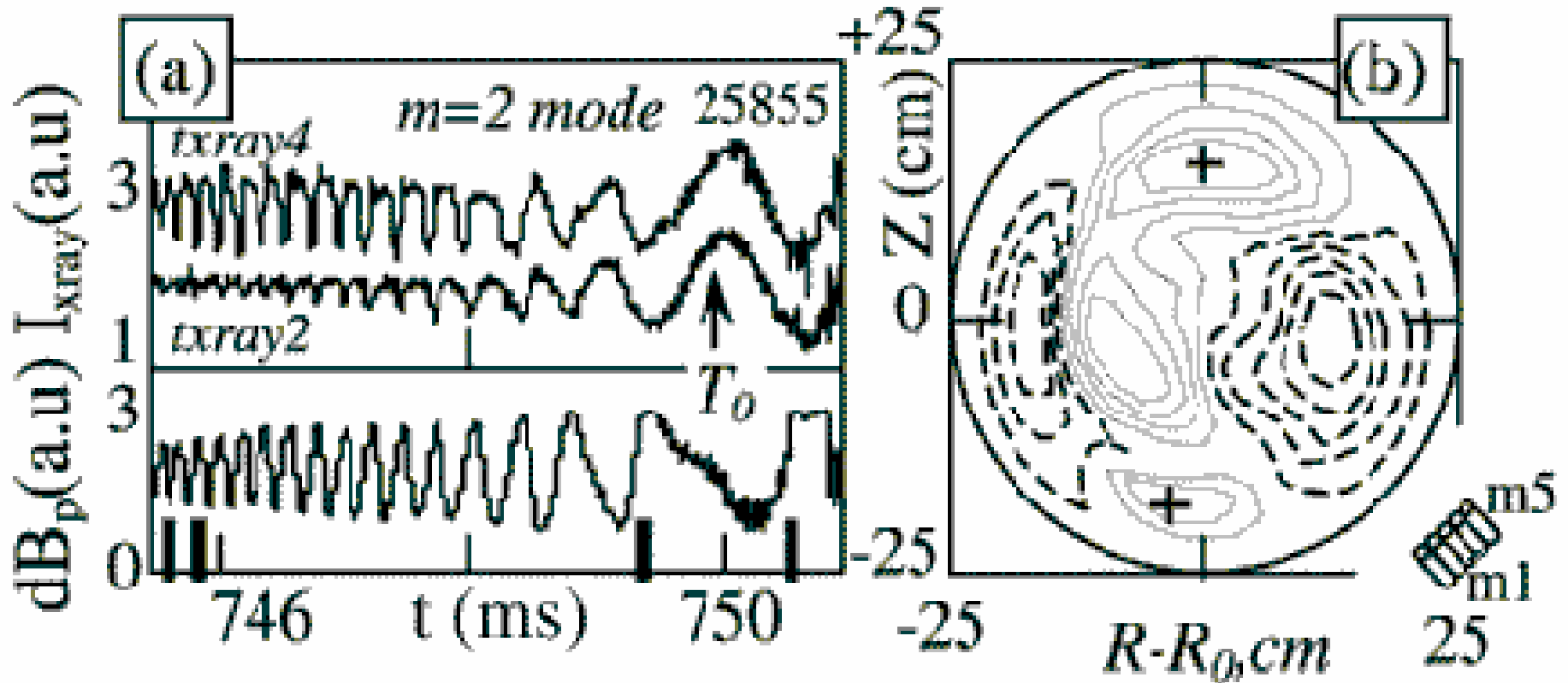


Coupling of the internal $m=1, n=1$ mode with the $m=2, n=1$ perturbations is observed just prior to the energy quench

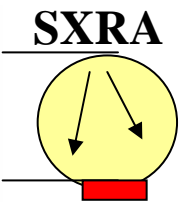
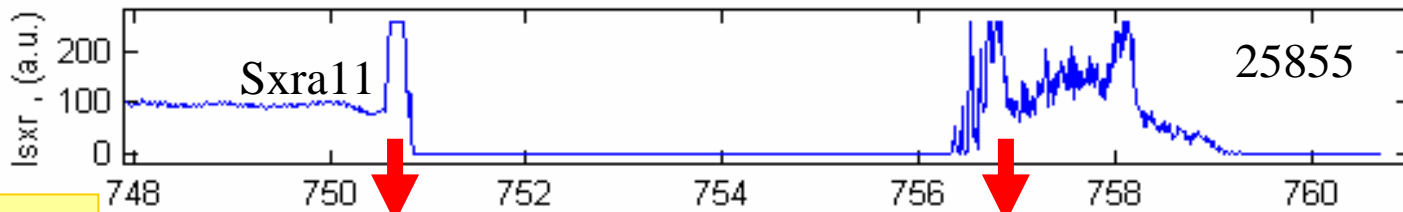




Position of the X-points of magnetic islands are identified from comparison of the x-ray images with data of fast magnetic probes

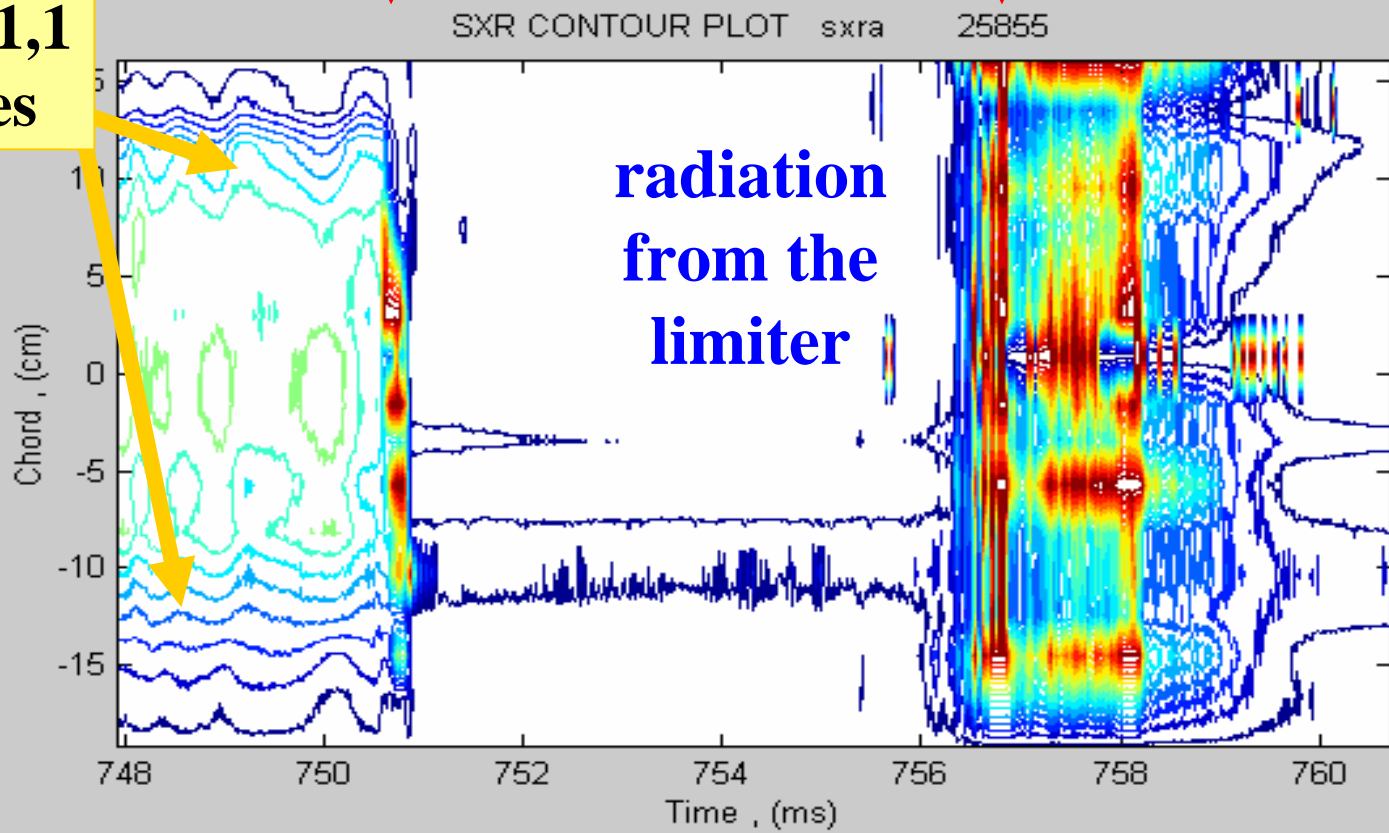


“Classical” hard x-ray bursts during density limit disruption



T-10

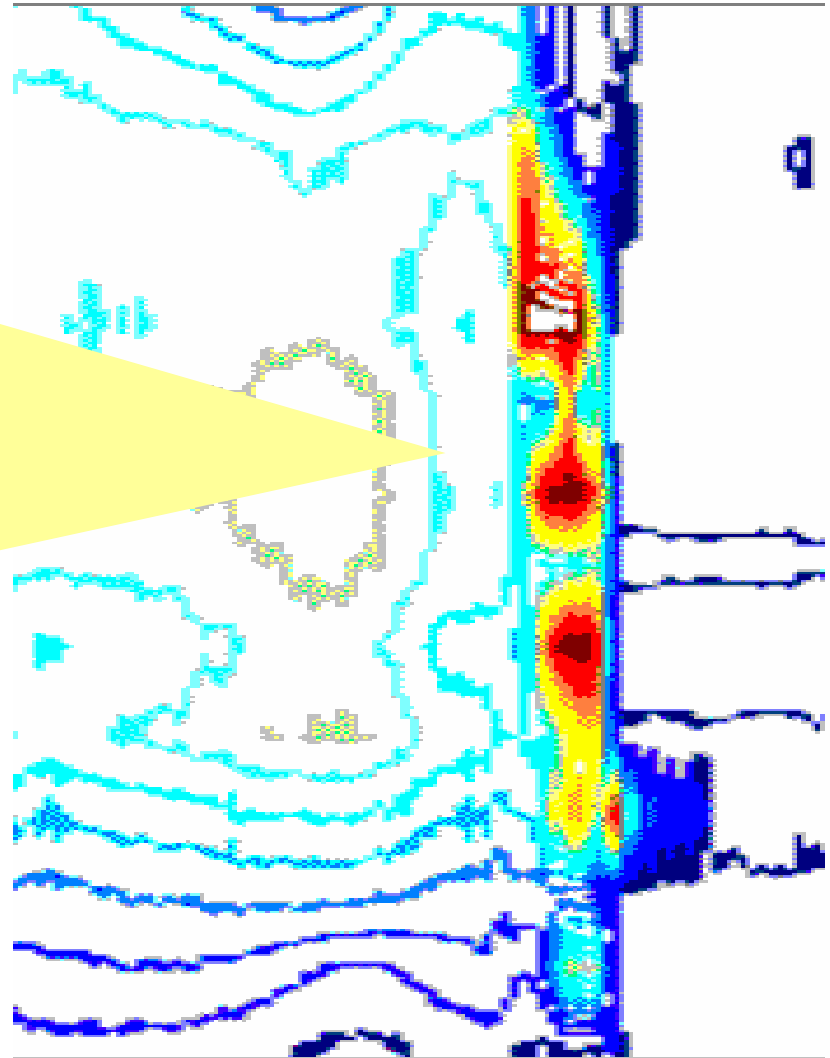
2,1 & 1,1 modes



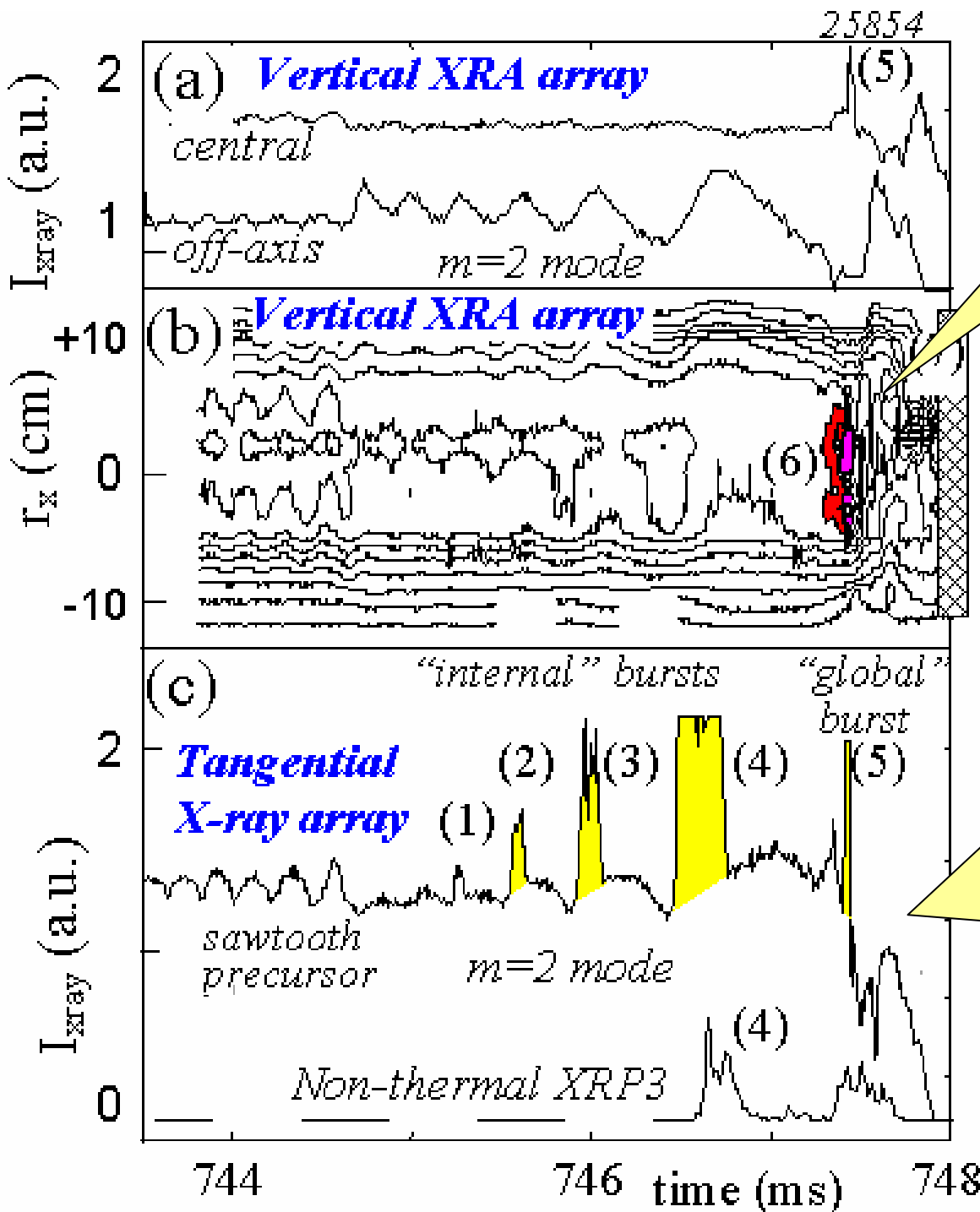
Rail Limiter

“Classical” hard x-ray burst

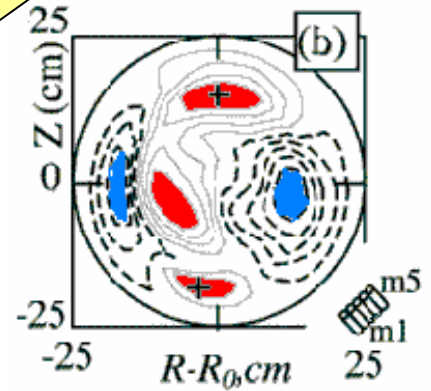
Narrow spots at the limiter can indicate filament-like structure of the beams - possibly connected with MHD modes?
see, also JET disruptions
[Gill,2000]



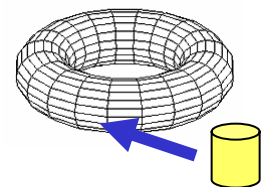
754 758 762 766
Time, (ms)



Standard x-ray spike



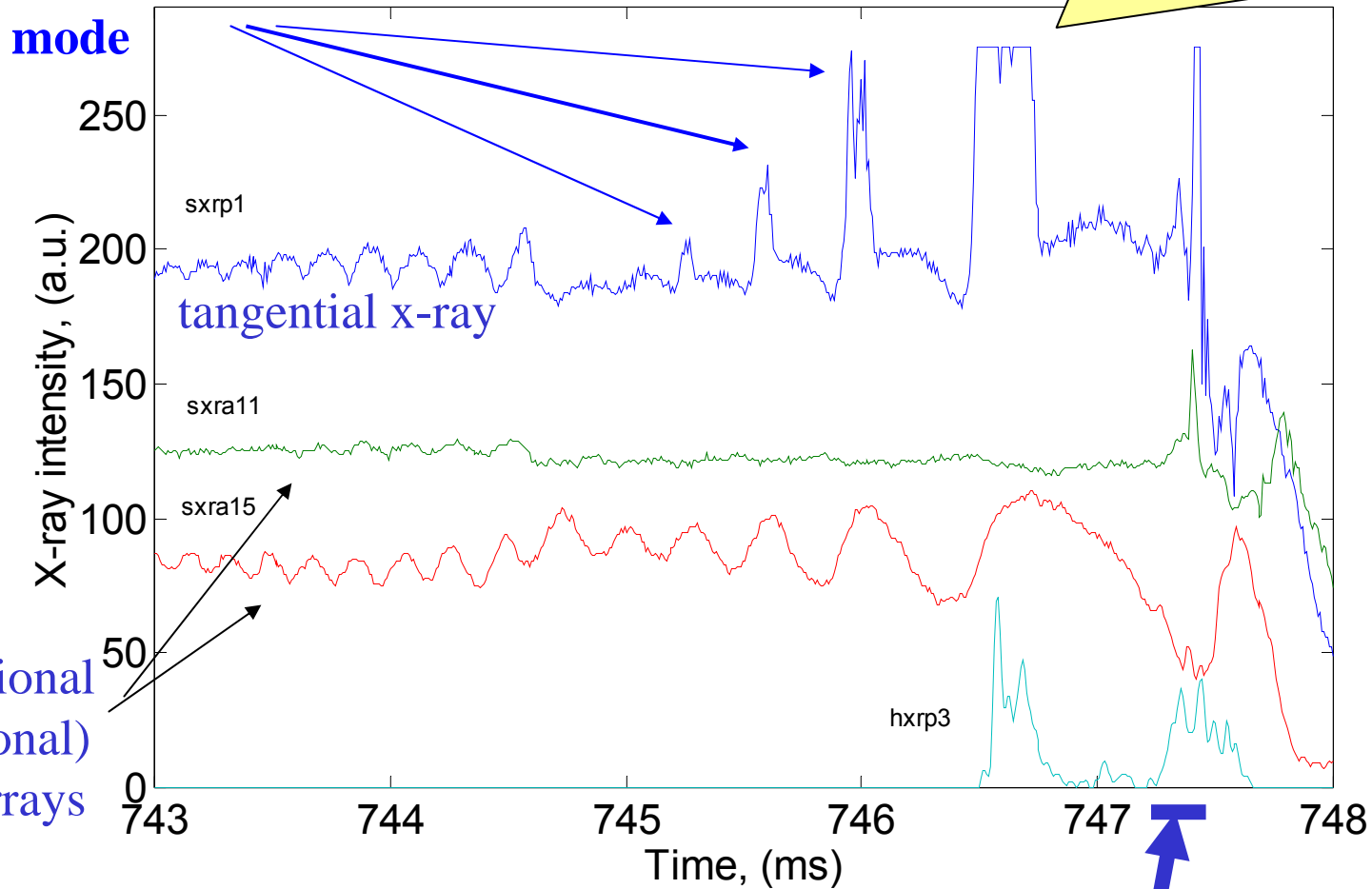
“Internal” x-ray bursts are observed with the tangentially viewing x-ray array





The x-ray bursts are observed at specific phase of the 2/1 MHD mode

The bursts can be connected with non-thermal electrons generated around the $m=2$ magnetic island



Standard x-ray burst during energy quench is observed with all x-ray arrays



SUMMARY

STAGE- 1



The pre-disruptive plasma is characterized by joint rotation of the coupled $m=1, n=1$ and $m=2, n=1$ MHD perturbations.



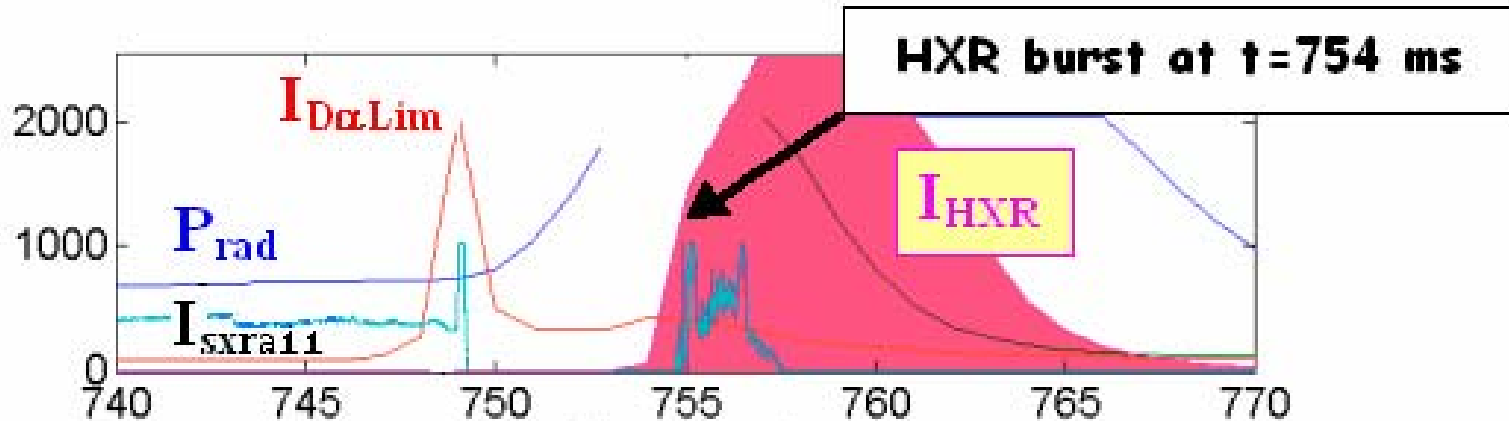
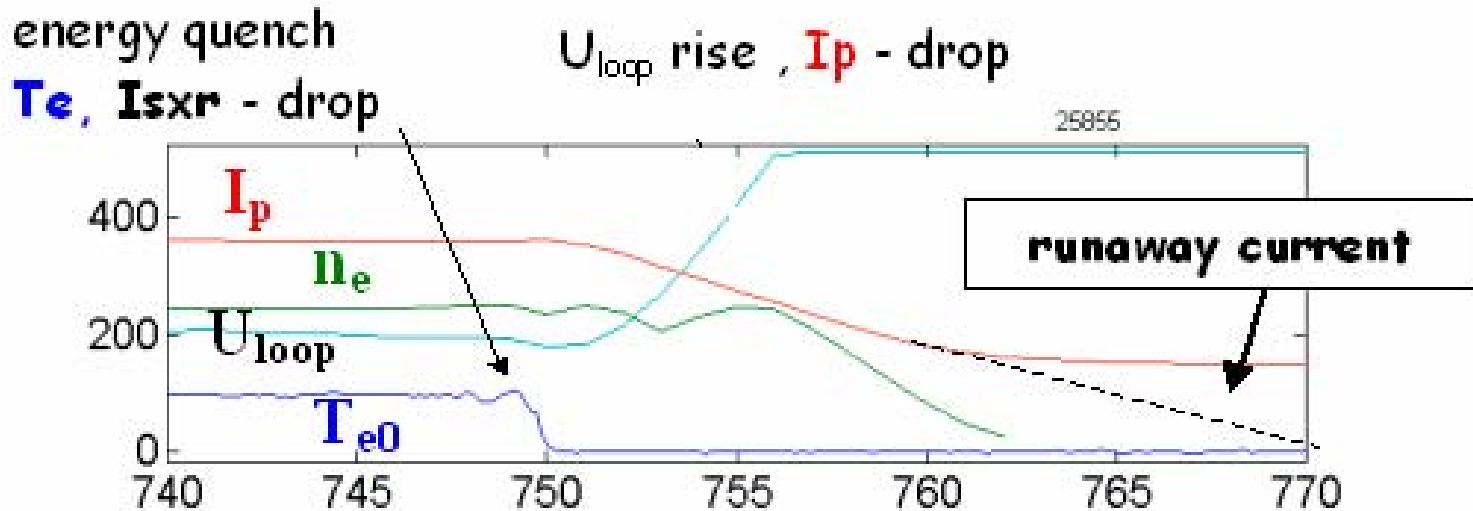
Non-thermal x-ray spikes are observed around X-points of the $m=1, n=1$ and $m=2, n=1$ magnetic islands just prior to the energy quench.



First non-thermal x-ray spike during an energy quench can be connected with interaction of the MHD-induced localized beams with the limiter.



Standard hard x-ray burst are observed 5ms AFTER the energy quench during runaway interaction with the “wall”

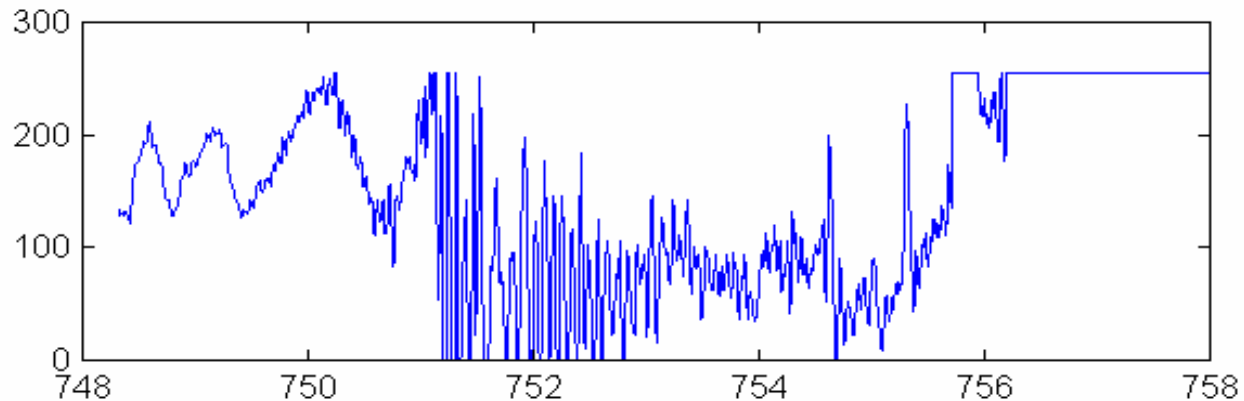
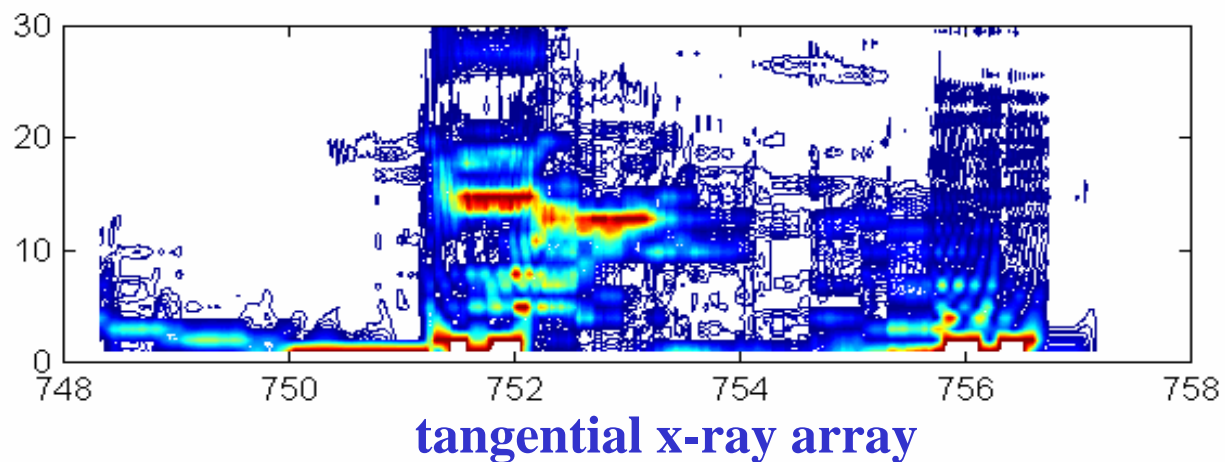
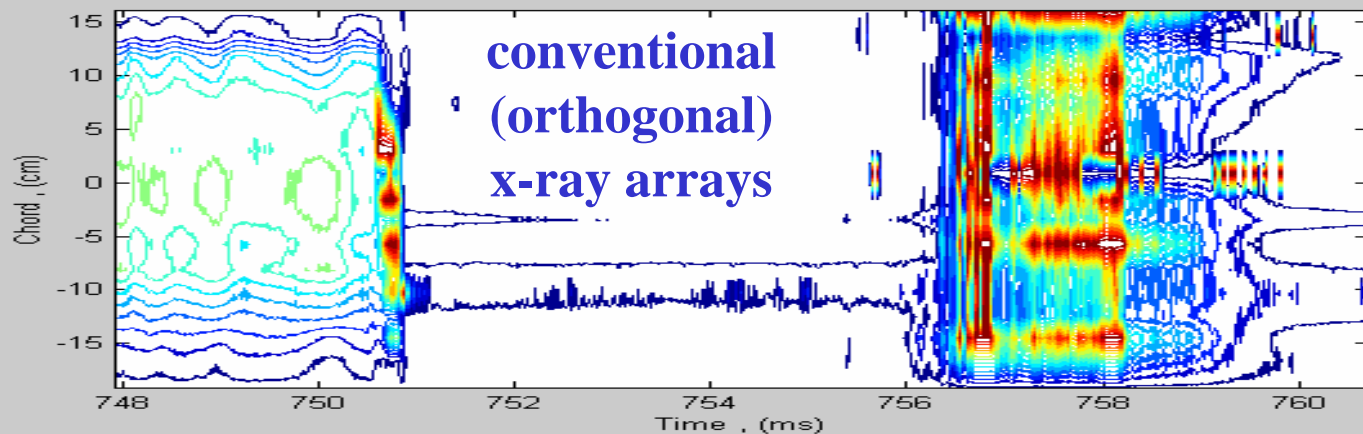


Time (ms)

Stage I pre-disruptive

Stage II energy quench and runaway formation

Stage III runaway avalanche



**x-ray bursts
are observed
with the
tangentially
viewing x-ray
array just
after an
energy
quench**

Nonthermal x-ray bursts after an energy quench are observed using tangentially viewing x-ray array

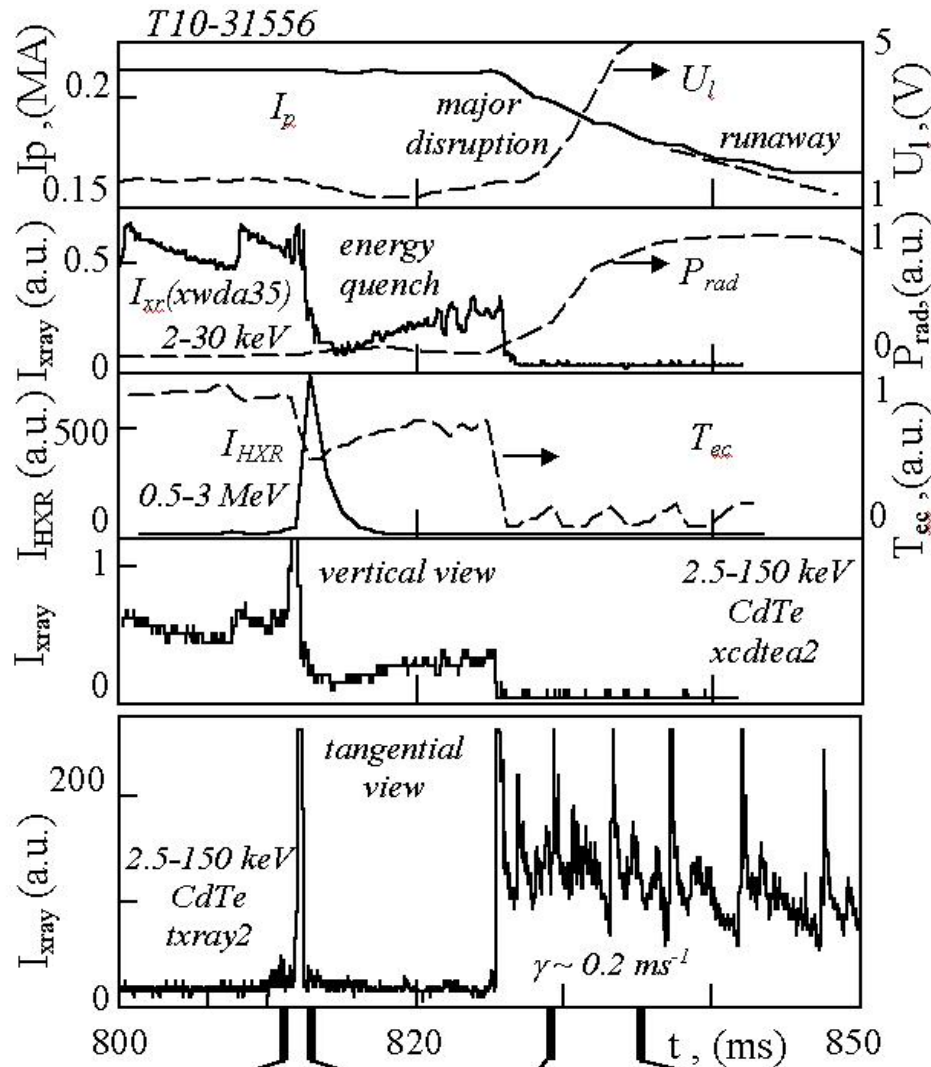
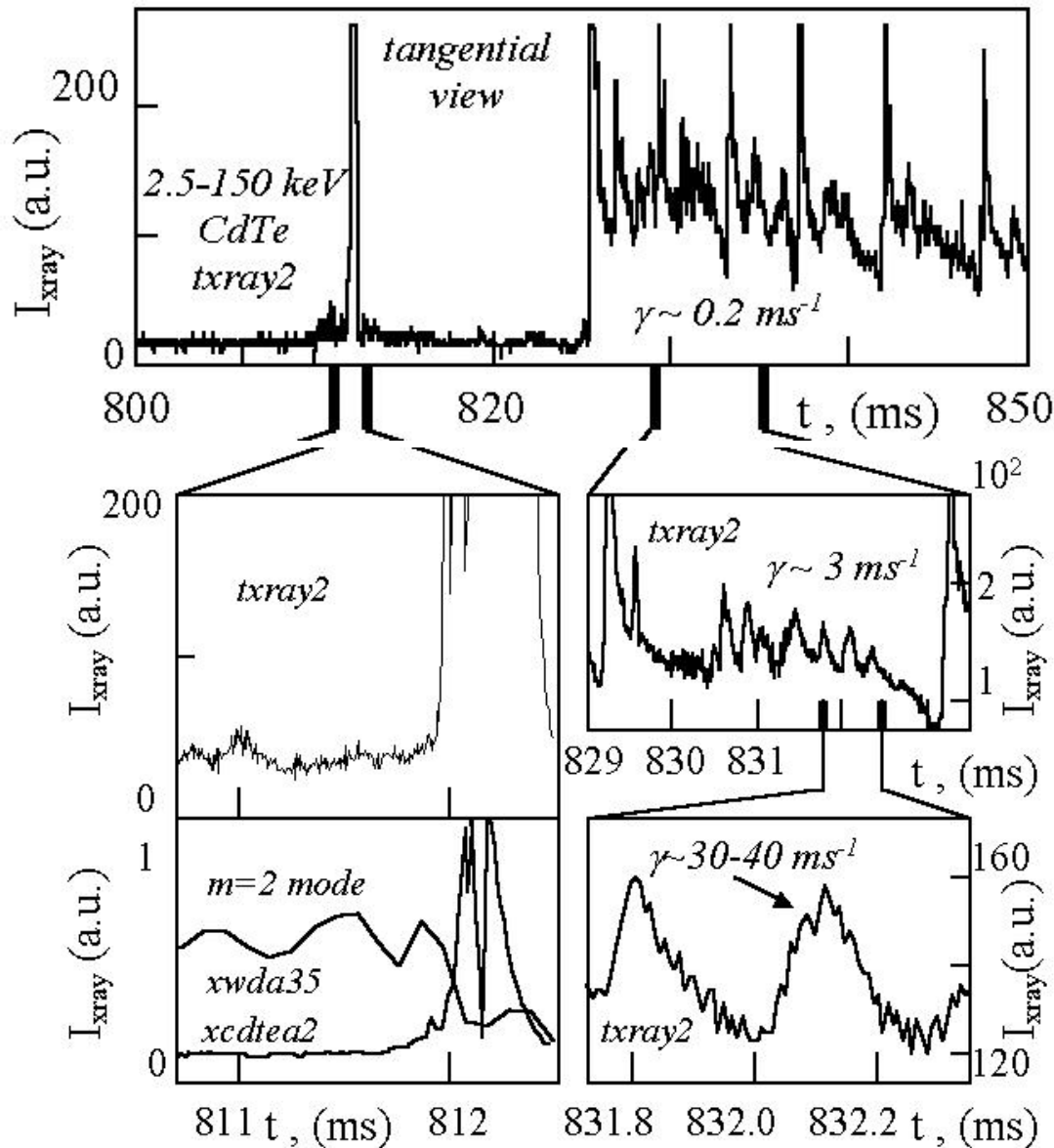


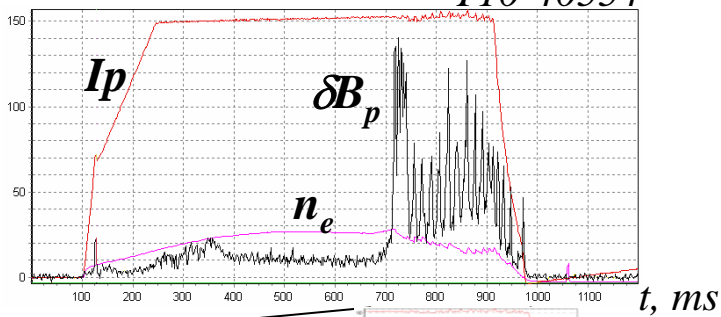
FIG. 12. Time evolution of plasma parameters after an energy quench during density limit disruption in ohmically heated plasma. Here, I_p is plasma current, U_l loop voltage, P_{rad} total radiated power, T_{ec} electron (ECE) temperature, I_{HXR} hard x-ray intensity, $I_x(xwda35)$ x-ray intensity measured using XWDA gas detector. Also shown, intensity of the x-ray radiation measured using CdTe detectors with orthogonal (*xcdtea2*) and tangential (*txray2*) view of the plasma column.

Nonthermal x-ray bursts after an energy quench are characterised by multiple frequencies

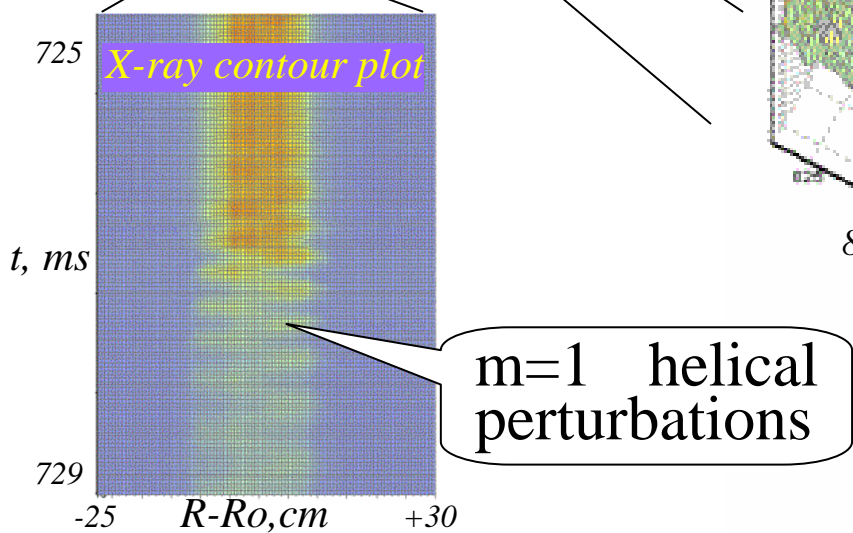
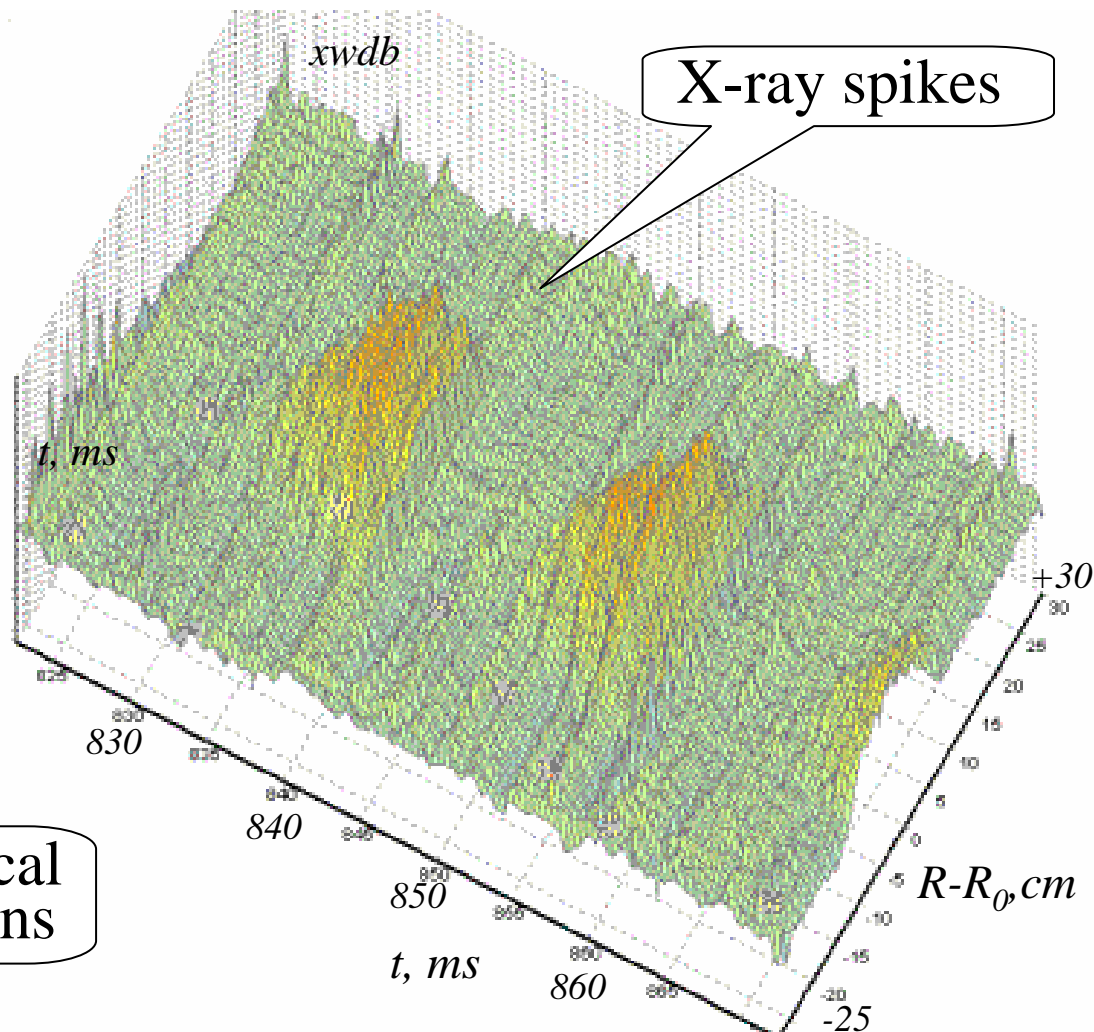
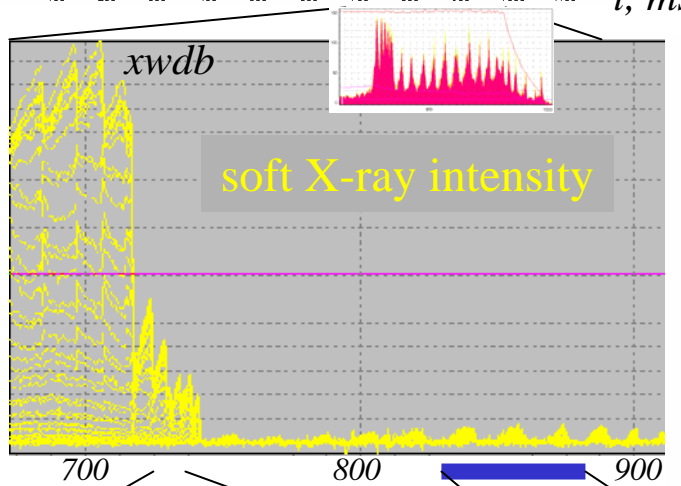


Note, some decrease in the repetition rate in sequence of the bursts

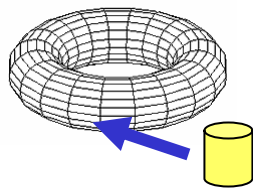
T10-40554



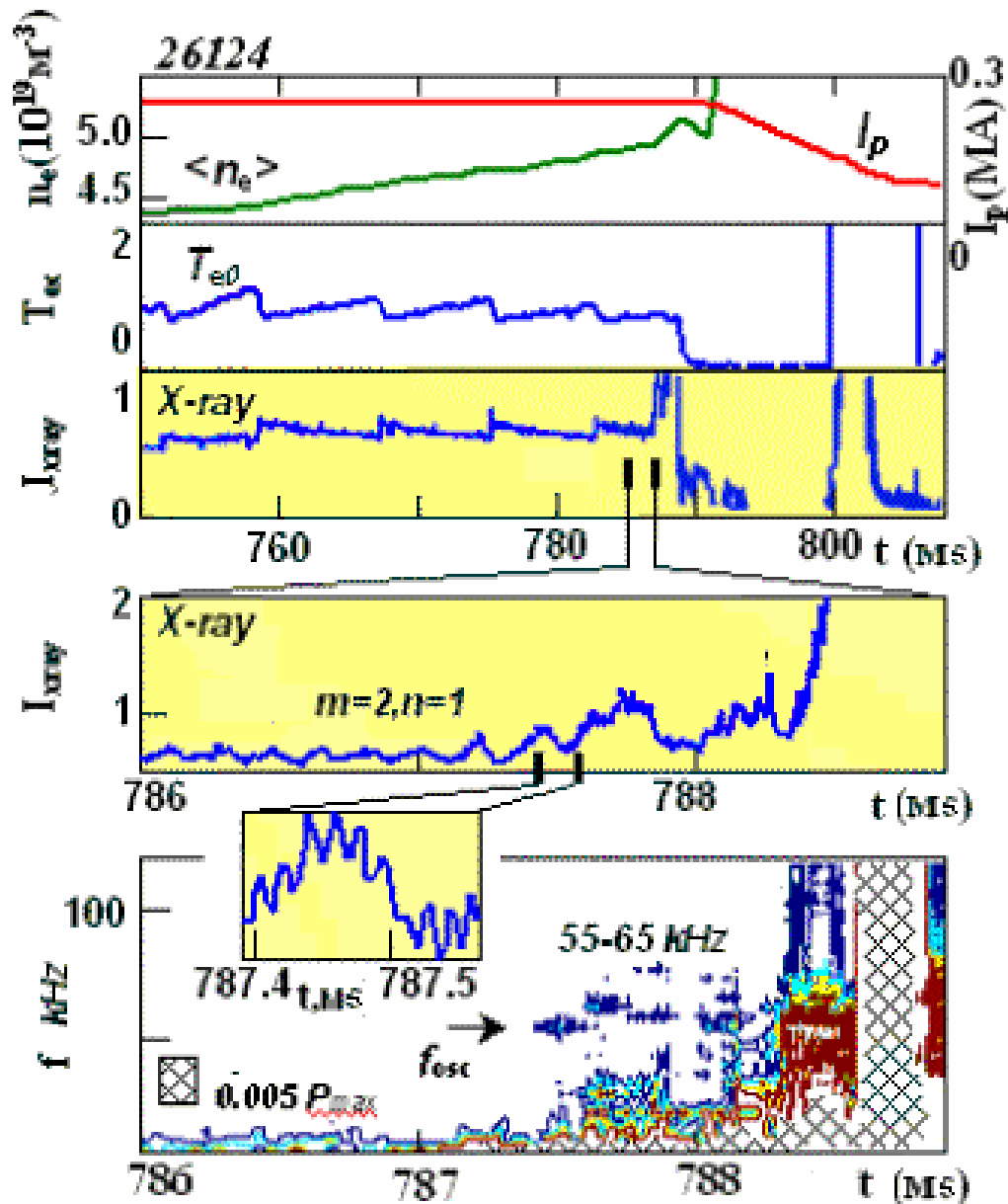
X-ray spikes after an energy quench can be localised around the same area as one of the $m=1$ helical perturbations



- Small-scale quasi-coherent oscillations ($f \sim 15\text{-}80\text{kHz}$) are observed prior to the density limit disruption using tangential view x-ray array

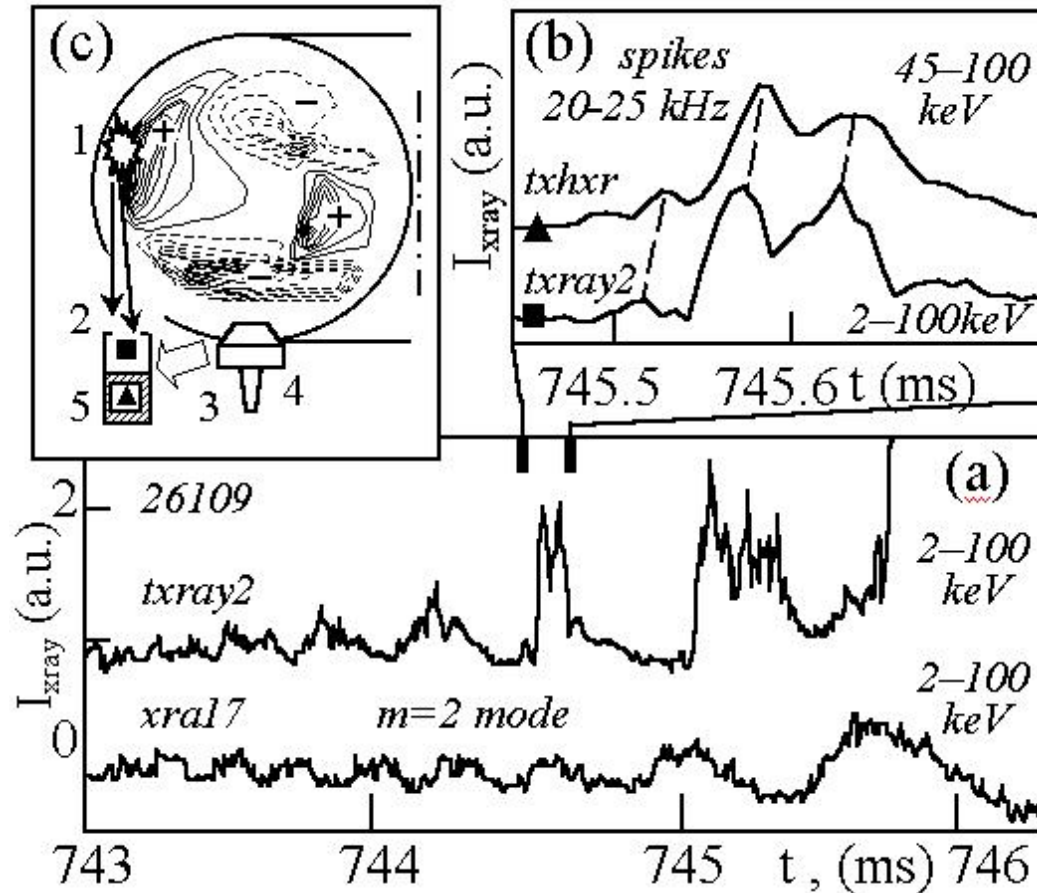


- Analysis indicated possible connection of the oscillations with beams of the non-thermal electrons induce during growth of the MHD modes

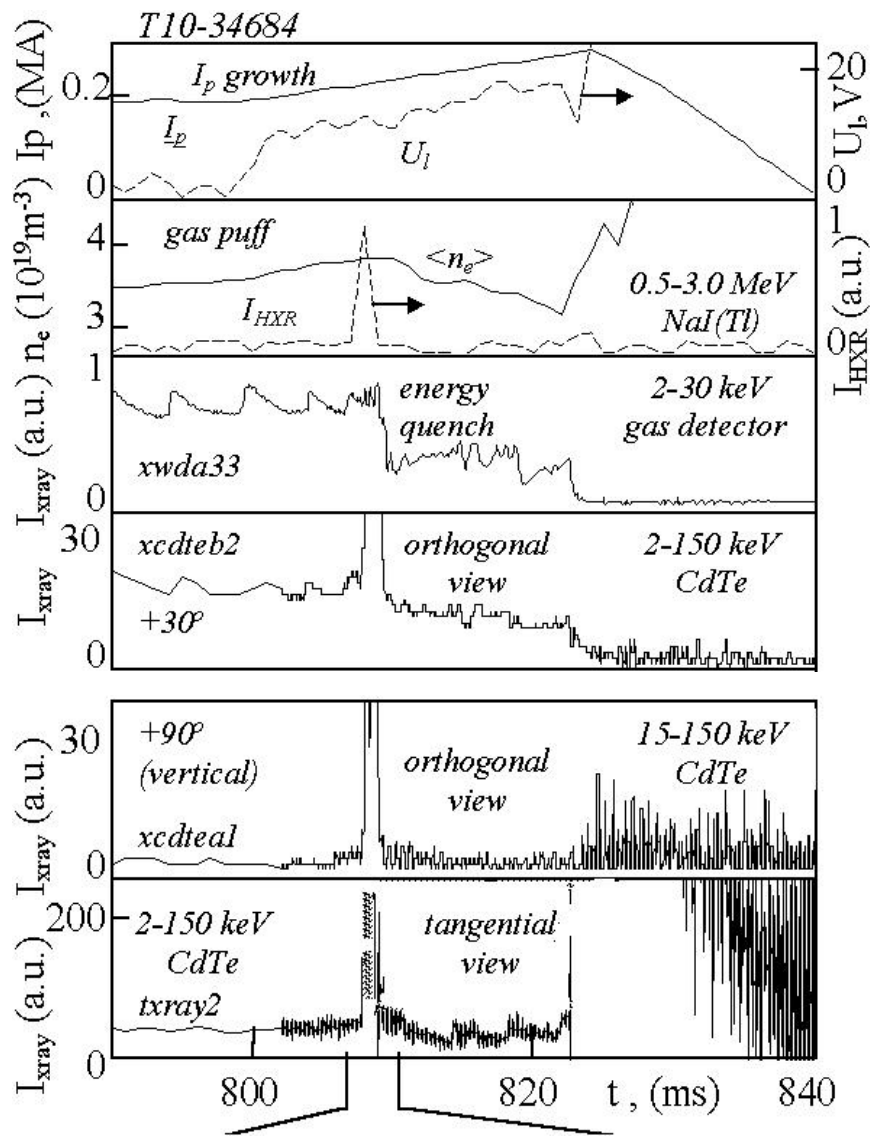




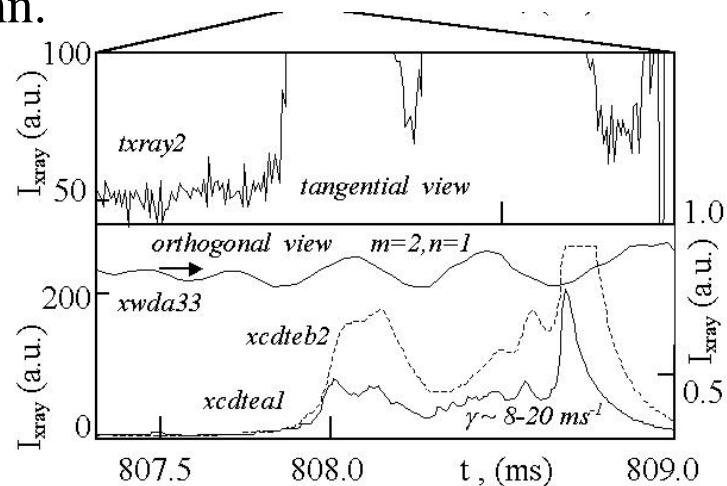
During the energy quench the quasi-coherent perturbations are transformed to intensive bursts of the non-thermal x-ray radiation with amplitude modulation in the same frequency range as one just prior to the disruption.



Experiments with the current ramp-up just prior to the disruption: No strong modification in the bursts behaviour



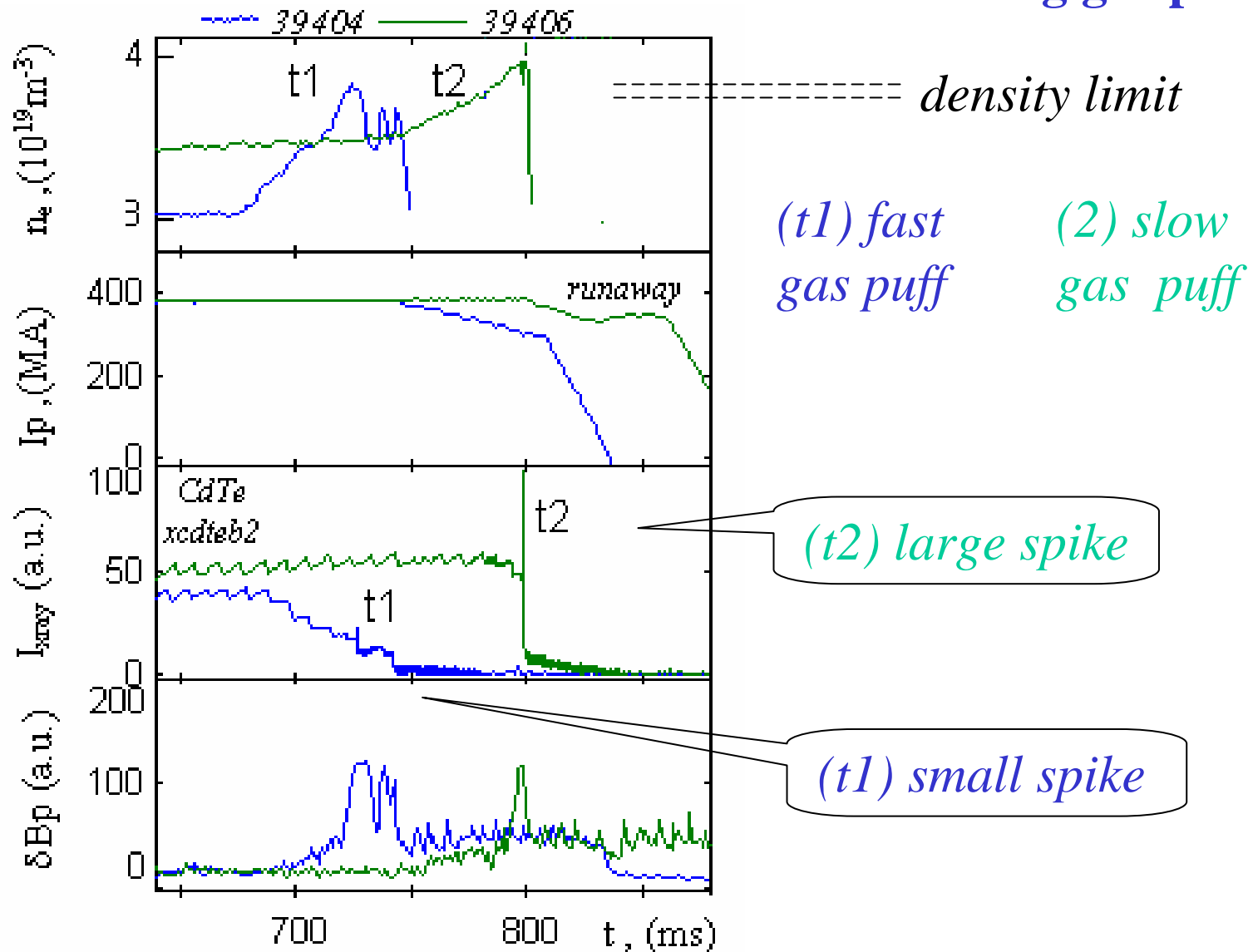
Time evolution of plasma parameters in experiments with ramp-up of plasma current, I_p , just prior the density limit disruption. Here, U_1 is loop voltage, $\langle n_e \rangle$ line averaged electron density, I_{HXR} hard x-ray intensity, $I_{\text{xray}}(\text{xwda33})$ x-ray intensity measured using XWDA gas detector. Also shown, intensity of the x-ray radiation measured using CdTe detectors with orthogonal (*xcdteal*, *xcdteb2*) and tangential (*txray2*) view of the plasma column.





Amplitude of the non-thermal x-ray spikes at the first minor disruption can be reduced up to 5-15 times in plasma with strong gas puffing

strong gas puffing





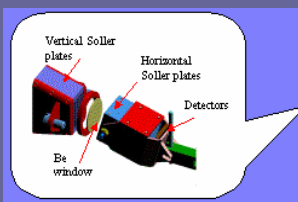
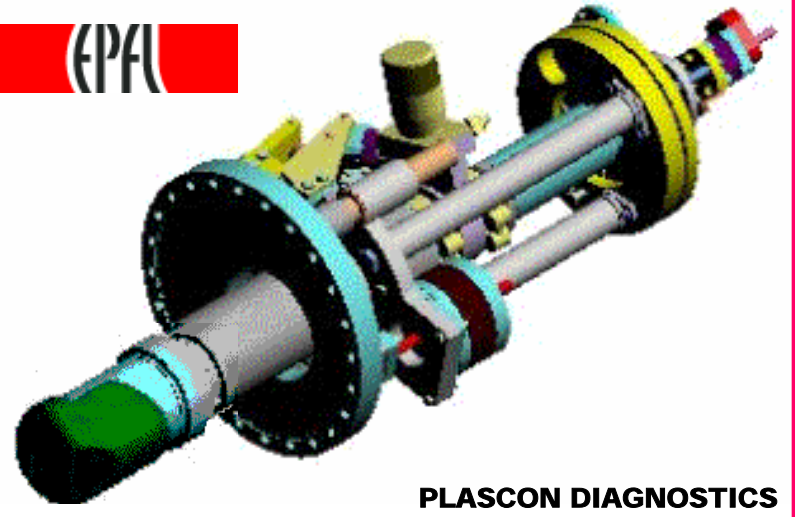
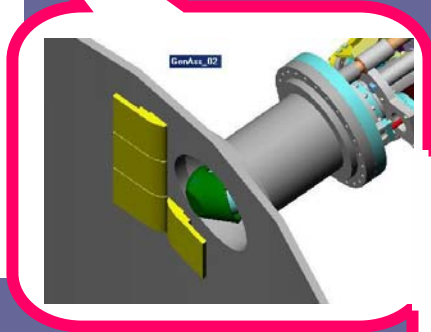
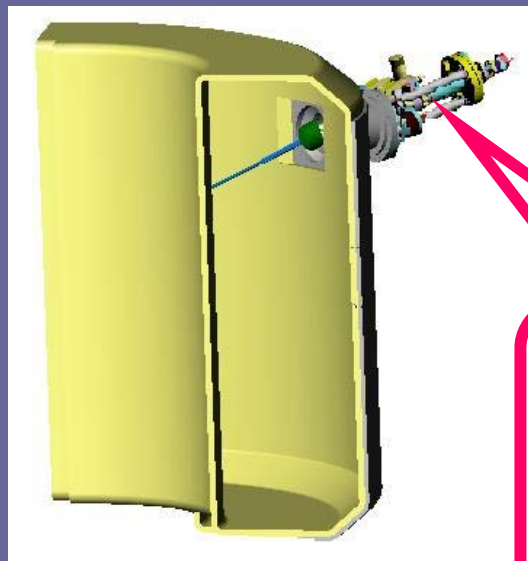
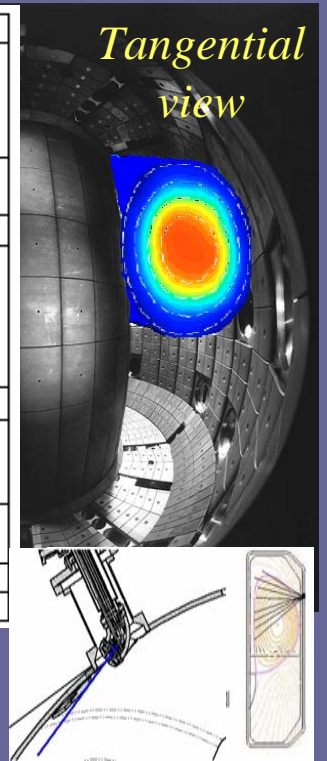
SUMMARY STAGE II

-  During the energy quench the quasi-coherent perturbations are transformed to intensive bursts of the non-thermal x-ray radiation with amplitude modulation in the same frequency range as one just prior to the disruption.
-  The x-ray bursts observed just after the energy quench are confined within the plasma core.
-  Strong increase of the longitudinal electric field prior to the disruption does not change considerably dynamic of the bursts. This indicates indirectly that bursts can not be connected with standard “equilibrium” runaway beams in the plasma core.
-  New diagnostics are required for future analysis.



New tangential X-Ray Detector Array Diagnostic system -measurements of the nonthermal x-ray radiation and small-scale MHD modes in the TCV tokamak

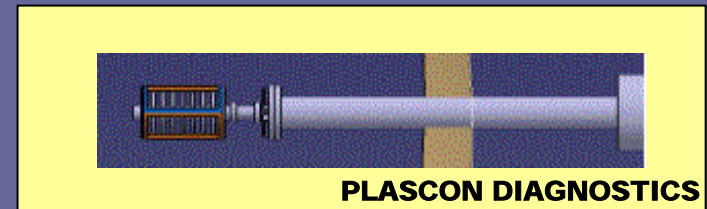
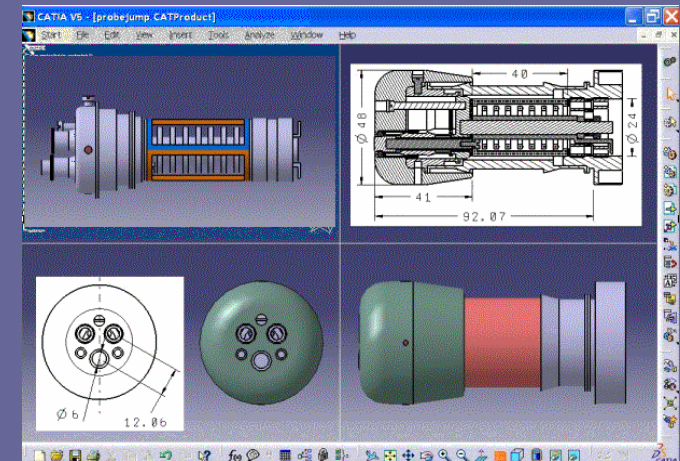
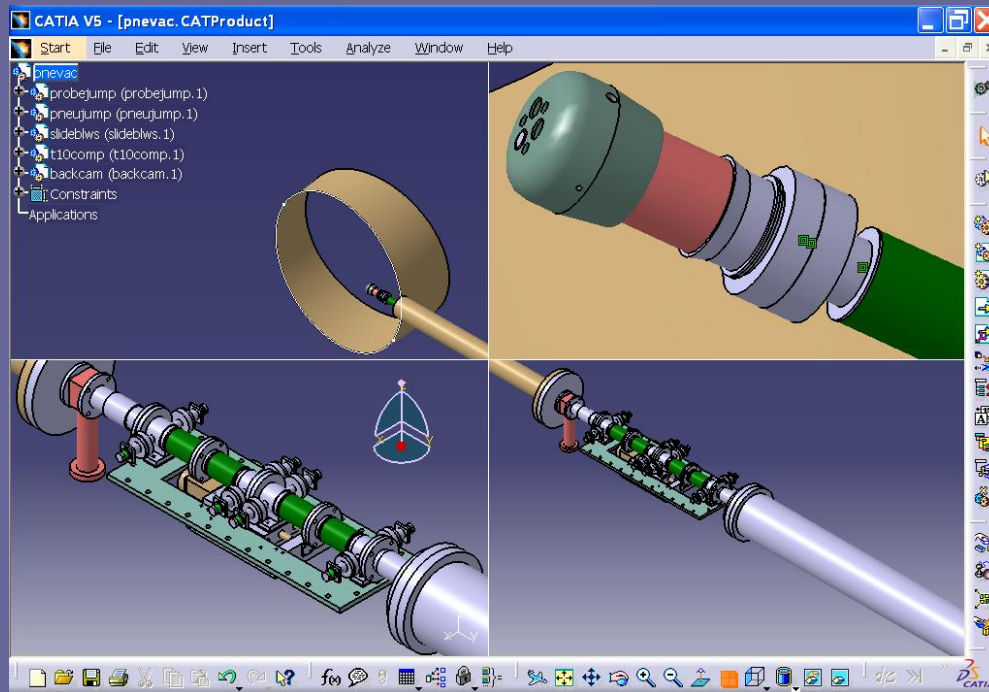
Port	upper lateral port CF200
Detectors CdTe	5 (+1 screened)
sensitive area	25 mm ² (5x5 mm)
sensitive region	d = 2 mm
thickness	
Energy range of the x-ray fluxes	E ~ 1.5 - 200 keV
Spatial resolution	dr ~ 2cm
Field of view of the diagnostic (can be changed in subsequent pulses by an automatic orientation system)	0 to -30° vertical direction 0 to 72° toroidal direction
Time resolution	dt ~ 0.01 msec
Baking temperature (after extraction of the detector array)	450°C
Helium Mass Spectrometer leak tight	1x10 ⁹ atm-cm ³ /sec
Electrical isolation	minimum 6 kV
Heat flux protection	Carbon composite



- CdTe detectors (2-200keV)
- Field of view is adjusted using two sets of a movable Soller collimators (0 - 70° toroidal, -15° - +15° vertical angle)

T-10 XEMERA probe:

1. Tangential X-ray with adjustable line-of-sight
2. Reciprocating Electric (Langmuir) probe
3. Fast reciprocating Magnetic probe



Acknowledgements

The author would like to thank A.Ya. Kislov, G.E. Notkin, Y.D. Pavlov and V.S. Strelkov for support of the experiments and Yu.N. Dnestrovskij, S.V. Mirnov, V.I. Poznyak, K.A. Razumova, I.B. Semenov and V.A. Vershkov for a critical discussion of the experimental results. Measurements of the hard x-ray monitor were kindly provided by A.V. Khramenkov.

Presentation of the paper at the 9th Technical Meeting on Energetic Particles is made possible due to generous support by the International Atomic Energy Agency.